SANDIA REPORT
SAND2022-15184
Printed October 2022

Sandia National Laboratories

Reconfiguration of the Respiratory Tract Microbiome to Prevent and Treat *Burkholderia* Infection

Steven Branda (8623; PI), Nicole Collette (LLNL), Nicole Aiosa (GIT), Neha Garg (GIT), Catherine Mageeney (8621), Kelly Williams (8623), Ashlee Phillips (LLNL), Kelsey Hern (UC-B), Adam Arkin (UC-B), Bryce Ricken (8631), Delaney Wilde (8623), Sahiba Dogra (8623), Brittany Humphrey (8631), Kunal Poorey (8623), Colleen Courtney (8621)

Prepared by
Sandia National Laboratories
Albuquerque, New Mexico
87185 and Livermore,
California 94550

Issued by Sandia National Laboratories, operated for the United States Department of Energy by National Technology & Engineering Solutions of Sandia, LLC.

Available to DOE and DOE contractors from
U.S. Department of Energy
Office of Scientific and Technical Information
P.O. Box 62
Oak Ridge, TN 37831

Telephone: (865) 576-8401
Facsimile: (865) 576-5728
E-Mail: reports@osti.gov
Online ordering: http://www.osti.gov/scitech

Available to the public from
U.S. Department of Commerce
National Technical Information Service
5301 Shawnee Rd
Alexandria, VA 22312

Telephone: (800) 553-6847
Facsimile: (703) 605-6900
E-Mail: orders@ntis.gov
Online order: https://classic.ntis.gov/help/order-methods/

ABSTRACT

New approaches to preventing and treating infections, particularly of the respiratory tract, are needed. One promising strategy is to reconfigure microbial communities (microbiomes) within the host to improve defense against pathogens. Probiotics and prebiotics for gastrointestinal (GI) infections offer a template for success. We sought to develop comparable countermeasures for respiratory infections. First, we characterized interactions between the airway microbiome and a biodefense-related respiratory pathogen (*Burkholderia thailandensis*; Bt), using a mouse model of infection. Then, we recovered microbiome constituents from the airway and assessed their ability to re-colonize the airway and protect against respiratory Bt infection. We found that microbiome constituents belonging to *Bacillus* and related genuses frequently displayed colonization and anti-Bt activity. Comparative growth requirement profiling of these *Bacillus* strains *vs* Bt enabled identification of candidate prebiotics. This work serves as proof of concept for airway probiotics, as well as a strong foundation for development of airway prebiotics.

CONTENTS

LIST OF FIGURES

LIST OF TABLES

This page left blank

ACRONYMS AND TERMS

Acronym/Term	Definition
GI	gastrointestinal
Bt	*Burkholderia thailandensis*
DOE	Department of Energy
DoD	Department of Defense
DHS	Department of Homeland Security
HHS	Department of Health and Human Services
CDC	Centers of Disease Control
rRNA	ribosomal RNA
NGS	next generation sequencing
GIT	Georgia Institute of Technology
UC-B	University of California at Berkeley
CFU	colony-forming units
OPA	oropharyngeal aspiration
PBS	phosphate buffered saline
DNA	deoxyribonucleic acid
LB	Luria broth
CP	candidate probiotic
T6SS	type VI secretion system
CDI	contact-dependent growth inhibition
sSputum	synthetic sputum
MLD	minimum lethal dose
PM	Phenotype Microarray
AU	arbitrary unit
NA	not applicable
ND	not done
Bs	*Bacillus subtilis*

1. INTRODUCTION

New approaches and tools for preventing and treating infectious diseases, particularly those originating in the respiratory tract, are sought by federal agencies tasked with countering weapons of mass destruction and ensuring soldier and citizen health (*e.g.*, DOE, DoD, DHS, HHS, CDC). One strategy that has garnered interest in recent years is to reconfigure microbial communities (microbiomes) within the host in order to improve their ability to competitively exclude, directly attack, and/or enlist host defenses against the infectious agent. In concept, this approach should avoid two crippling drawbacks of antibiotics: 1) Inevitable development of resistance; and 2) Profound destruction of resident microbiomes, which renders the host vulnerable to secondary infections as well as other disorders.

Thus far, virtually all attempts to implement this approach have focused on reconfiguration of microbiomes resident to the GI tract. This is largely due to the long and fraught history of attempting to prevent/treat GI disorders by ingesting prebiotics (nutrient supplements designed to feed beneficial microbiome constituents *in situ*) and probiotics [beneficial constituents (or surrogates) themselves] in order to address the dysbioses thought to cause the disorders. The bias has been self-reinforcing, in that most of the methods, tools, and specialized knowledge (*e.g.*, microbiome composition data) that support prebiotics/probiotics development have been designed with the GI application space in mind. Nevertheless, in recent years the prebiotics/probiotics approach to combating GI disorders, including infectious disease, has proven effective; and with the advent of high-throughput molecular biology [particularly 16S ribosomal RNA (rRNA) profiling *via* next generation sequencing (NGS)], synthetic biology, and culture of undomesticated microbes, there is new opportunity and interest in applying these approaches to other contexts, including the respiratory tract (**Figure 1**). Additionally, the impressive advances in synthetic biology have opened up a new direction in medicine: Development of "living countermeasures", in which cells genetically engineered to recognize and respond to stimuli of interest are used as sensors (for diagnostic applications) and context-triggered delivery vehicles (for therapeutics, antigens, and adjuvants) *in situ*. This concept has been extended to applications in agriculture and ecology as well. In a few cases, proof of principle has been demonstrated for the utility in equipping probiotic microbes with heterologous means of selectively and directly attacking the pathogen in order to better prevent or mitigate infectious disease; predictably, all of these cases were limited to the GI application space. Practitioners at the forefront of this field are developing methods and tools that enable facile design, assembly, modification, introduction, and testing of heterologous genetic circuits in virtually any microbe, such that development of a synthetic biology platform for constructing programmable probiotics (*i.e.*, sets of standardized circuit components and receptive host microbes that can be combined and shuffled at will to alter without destroying function) is now possible.

Taking advantage of these new developments, and bringing to bear our expertise in host-pathogen interactions (particularly those of bacterial pathogens of biodefense concern, and analysis of them using mouse models of respiratory infection); microbiome, transcriptome, and (through our collaboration with GIT) metabolome analyses; molecular biology; and culture of undomesticated microbes; we sought to:

- Characterize the interaction between a biodefense-related bacterial pathogen (Bt) and the respiratory tract microbiome in a mouse model of respiratory infection; and
- Rationally manipulate these interactions, though prebiotic and probiotic approaches, to prevent and treat respiratory infection.

Our central hypothesis was that enhancement of the resident airway microbiome using prebiotics/probiotics can confer protection against respiratory infection. We investigated this idea by addressing the following Specific Aims:

- Aim 1: Characterize the airway microbiome in healthy *vs* infected mice.
- Aim 2: Enhance the airway microbiome using prebiotics and probiotics.

Our original proposal included a third Specific Aim (to develop programmable probiotics for prevention/treatment of respiratory infection) that ultimately was not pursued in the context of this project.

This report summarizes our efforts to address these Specific Aims, the results that they yielded, the implications of our results, and our perspective on potentially productive future directions.

It should be noted that as an initial step in profiling changes in secondary metabolite production associated with respiratory Bt infection, our collaborators at GIT carried out metabolomic profiling studies of relevant cell types (airway epithelial cells and macrophage) infected with Bt *in vitro*. These studies are not described in this SAND report, but rather in a peer-reviewed publication [1].

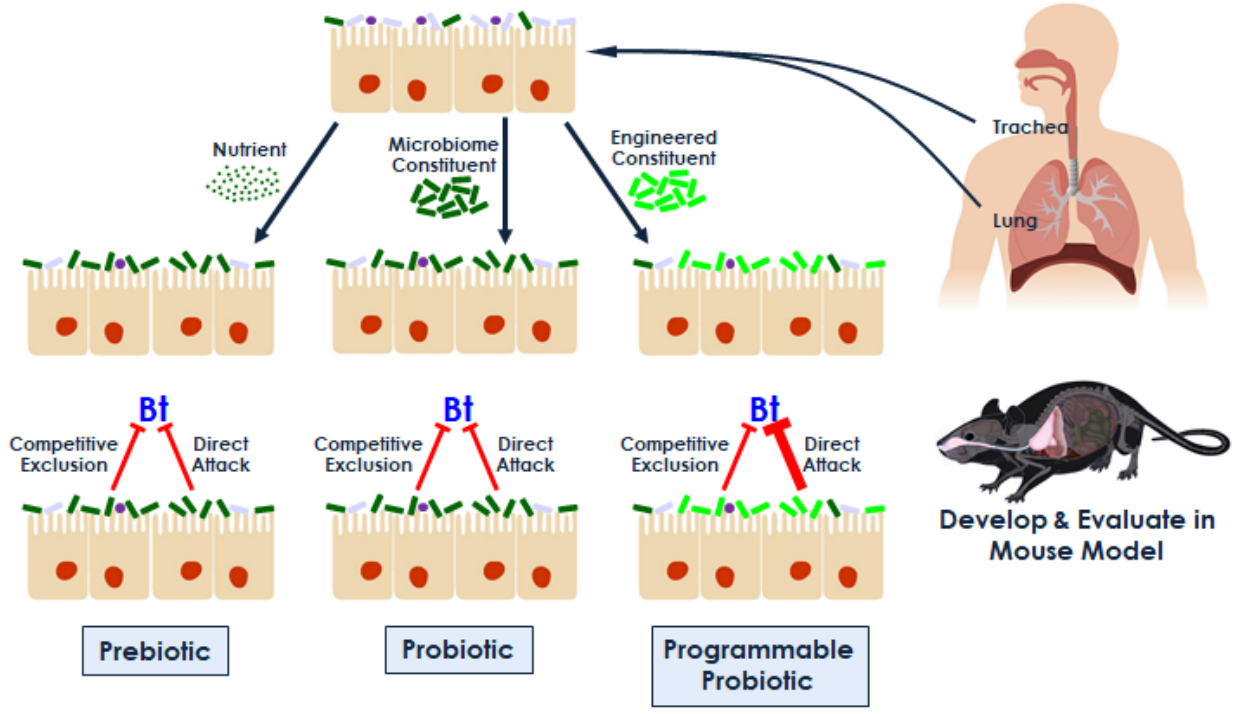

Figure 1. Overview of Airway Microbiome Manipulation Strategies. Prebiotic approach (left): Supplement airway with nutrients designed to feed beneficial microbiome constituents *in situ*. Probiotic approach (center): Recover beneficial microbiome constituents into culture, expand, then re-introduce into airway. Programmable probiotic approach (right): Recover beneficial (or neutral) microbiome constituents into culture, equip with a genetic contruct designed to enhance colonization and/or anti-infection activity, expand, then re-introduce into airway.

2. AIM 1: CHARACTERIZE THE AIRWAY MICROBIOME IN HEALTHY *VS* INFECTED MICE.

Every mammalian body compartment that opens to the external world features a complex yet roughly stable microbiome. The respiratory tract is no exception: The human oral and nasal microbiomes are well characterized, and recent studies indicate that, contrary to conventional wisdom, even the lower airways and lungs are stably colonized by bacteria. Pathogens entering the respiratory tract must encounter its microbiomes almost immediately, prior to or coincident with interaction with host cells (*e.g.*, airway epithelial cells, macrophages); yet far less is known about the pathogen/microbiome interactions and their implications for respiratory infection. A better understanding of these interactions should enable us to rationally manipulate them for the benefit of human health.

2.1. 16S rRNA Profiling of Mouse Airway Microbiome - Literature Data.

As a precursor to our own 16S rRNA profiling effort (Section 2.2), we collected and analyzed publicly available data generated by previously reported efforts to characterize the airway microbiome in naive (uninfected). Data from 4 studies were used (**Table 1**) [2-5]. Phylogenetic placement of mapped reads was accomplished using an in-house bioinformatics pipeline (RapTOR). Each phylogenetic family was assigned a rank based on the prominence with which it was represented in a given dataset (*i.e.*, according to the relative abundance of mapped reads placed in the family); and its average rank calculated from the 4 individual dataset ranks. We found that 511 families were represented in all 4 datasets; the 25 of highest average rank are listed in **Table 2**.

2.2. 16S rRNA Profiling of Mouse Airway Microbiome - SNL Data.

In order to investigate the effects of infection on airway microbiome composition, we carried out 16S rRNA profiling studies of airway (trachea + lung) tissues recovered from naive *vs* Bt-infected C57Bl/6J mice. In parallel, we profiled liver and spleen tissues recovered from the same mice; these were expected to be essentially free of bacteria in the naive mice (thus serving as negative controls) but potentially loaded with Bt in the infected mice (due to dissemination from the airway).

For infections, Bt [$2x10^3$-$2x10^7$ colony-forming units (CFU) in 30 μl] was administered directly to the airway *via* oropharyngeal aspiration (OPA) [6]; and tissues were collected at pre-defined times: 1d post-Bt for $2x10^6$ and $2x10^7$ doses (mice were moribund); 3d post-Bt for $2x10^5$ doses (mice were moribund); and 5d post-Bt for $2x10^6$ and $2x10^7$ doses (mice were recovering). The tissues were homogenized in phosphate buffered saline (PBS), and DNA extracted from the homogenates to serve as template for 16S rRNA amplicon sequencing (96-plex library, MiSeq 300PE reads). Phylogenetic placement and enumeration of reads was accomplished using Kracken2 and Bracken software tools [7-9], running against RDP [10] at the family level and reporting only families represented in ≥50% of samples and/or accounting for ≥5% of mapped reads in any given sample.

Representative results from lung tissues (in this case analyzed separately from trachea) from Bt-infected mice are shown in **Figure 2**. As might be expected, we found that bacteria detected in the lungs predominantly belonged to the Burkholderiaceae family; phylogenetic analysis at the species level confirmed that these reads were derived from Bt. Setting aside these Bt-derived reads, the remaining reads mapped to a wide variety of families, predominantly Oxalobacteraceae, Neisseriaceae, Enterobacteriaceae, Comamonadaceae, Lactobacillaceae, Alcaligenaceae, and Bacillaceae, all of which are well represented in the airway microbiomes of naive mice (**Table 2**). Perhaps surprisingly, we

found that the relative proportions of reads mapping to these minority families varied little with Bt dose or collection time, an indication that Bt infection did not radically alter the core composition of the airway microbiome, despite overwhelming loads of Bt in the airway.

We attempted to further substantiate this finding by similarly analyzing airway homogenates from naive mice, but found that the 16S rRNA profiles were dominated by contamination that could be traced to multiple sources (primarily reagents and equipment, but also working surfaces and rooms). We were unable to resolve this problem, despite many attempts and extensive troubleshooting. In light of the results from profiling the tissues from Bt-infected mice, it seems likely that the problematic step was NGS library preparation, which was not carried out with enough DNA template to avoid jack-pot effects (runaway amplification of the few template molecules at hand, causing stochastic over-representation of these templates); this could be addressed by doping in a dummy template (Bt serves this role in the infected tissues) or combining airway DNA extracts from many mice before NGS library preparation.

In summary, at a gross level the phylogenetic composition of the airway microbiome was apparently resilient to Bt infection, but this observation must be considered preliminary due to the lack of high quality negative control data from study-matched uninfected mice.

2.3. Culturomic Profiling of Mouse Airway Microbiome.

In addition to 16S rRNA profiling, we carried out a culturomic profiling [11,12] effort, in which airway microbiome constituents were recovered into culture using a variety of preparative and growth conditions and then identified through genome sequencing (**Figure 3**). In these studies, airway tissues were collected from naive mice (24 in total), homogenized, and each homogenate (in 100 μl aliquots) used to inoculate:

- 5 different solid growth media [tryptic soy; tryptic soy + 5% sheep's blood; M9 minimal salts + 0.2% glucose; brain-heart infusion; and Luria broth (LB)].
- 3 different BACTEC blood bottles (Plus Aerobic/F; Plus Anaerobic/F; and Lytic/10 Anaerobic/F).

The inoculated solid growth media were incubated at 37°C for 7 d. The blood bottles were incubated at 37°C with shaking (250 rpm) for 1-5 d, and 100 μl aliquots periodically withdrawn for use in inoculating the 5 different solid growth media, which were then incubated at 37°C for 7 d. All colonies detected on the solid growth media (286 in total) were individually transferred to LB agar and, after further incubation at 37°C for 1-3 d, streaked to single colonies on LB agar. A representative single colony for each recovered microbiome constituent was used to inoculate LB liquid and solid media, incubated at 37°C for 1-3 d, and the bacteria used to generate a frozen glycerol stock (185 in total). Each isolate was then resuscitated from the frozen stock using LB liquid and solid media, and the viable isolates (159 in total) assessed for potential redundancy based on source material and growth characteristics (rate, dispersion/aggregation in liquid culture, colony morphology on solid media). Apparently non-identical isolates (101 in total) were analyzed by NGS [20- to 96-plex, NextSeq 150SE reads; coverage depth (reads/isolate): 2.1M average, 2.0M median, 34K - 6.9M range), using BBDuk (quality filtering and read trimming) [13] and SPAdes (assembly) [14] to generate contigs that were then aligned against genome sequences in RefSeq [15] for phylogenetic placement, which was called on the basis of alignment statistics for each assembly's contigs [genus match (contigs/assembly): 91.2% average, 100% median, 34.5% - 100% range; species match (contigs/assembly): 78% average, 87% median, 0.5% - 100% range]. All phylogenetic placements were confirmed using autoMLST [16]

and an in-house pipeline (speciate.pl) that calls MASH [17] and fastANI [18]. These analyses indicated that we had recovered 37 genetically-distinct airway microbiome constituents that belonged to 33 different species. Of the 37 isolates, 33 (89%) belonged to the 25 phylogenetic families most robustly represented in the mouse airway microbiome as determined through 16S rRNA profiling (Section 2.1) (**Figure 4**), a strong indication that the isolates did in fact originate in the airway rather than spurious interaction with it or from environmental contamination.

Report	Number of Mice	Mouse Strain	Mouse Age	Tissue Type(s)	Mapped Reads	Ave Reads/Sample	Reference
BMC Microbiol 13:303 '13	9	BALB/c	9 wk	lung	86.9K	9.7K	19
PLoS ONE 12:e0180561 '17	18	BALB/c	12 wk	upper lung, lower lung	6.6K	194	20
Microb Ecol 75:529 '18	35	BALB/c	1-36 wk	lung	677.7K	19.4K	21
Am J Respir Crit Care Med 198:497 '18	73	C57Bl/6J	8-10 wk	lung	527.2K	7.2K	5

Table 1. Samples and Data from Previously Reported 16S rRNA Profiling of the Mouse Airway Microbiome.

Family	Ave Rank
Lachnospiraceae	6.5
Streptococcaceae	7
Clostridiaceae	9
Comamonadaceae	10.75
Pseudomonadaceae	11.5
Bacillaceae	18.25
Staphylococcaceae	19
Enterobacteriaceae	20.25
Caulobacteraceae	22.5
Ruminococcaceae	22.75
Cytophagaceae	23.5
Oxalobacteraceae	24
Lactobacillaceae	25
Flavobacteriaceae	26
Sphingomonadaceae	26.25
Porphyromonadaceae	27
Moraxellaceae	27.25
Prevotellaceae	27.5
Xanthomonadaceae	28.5
Burkholderiaceae	28.75
Rhodobacteraceae	32.5
Microbacteriaceae	34
Micrococcaceae	34.25
Methylobacteriaceae	34.75
Desulfovibrionaceae	38.5
Bradyrhizobiaceae	38.75
Eubacteriaceae	39.75
Veillonellaceae	41
Neisseriaceae	41.25
Peptococcaceae	42.25
Peptostreptococcaceae	46.25
Erysipelotrichaceae	48.25
Pasteurellaceae	49.5
Micromonosporaceae	51.25
Corynebacteriaceae	52.25
Carnobacteriaceae	54
Sphingobacteriaceae	54.75
Rhizobiaceae	56.5
Hyphomicrobiaceae	57.75
Chitinophagaceae	58.25
Brucellaceae	59.25
Rickettsiaceae	60.5
Nocardiaceae	61.25
Bacteroidaceae	61.5
Coriobacteriaceae	61.5
Alcaligenaceae	63
Poaceae	63.5
Rhodocyclaceae	64.25
Acetobacteraceae	65.5
Peptoniphilaceae	70

Table 2. Phylogenetic Families Most Prominently Represented in Samples and Data from Previously Reported 16S rRNA Profiling of the Mouse Airway Microbiome. Data were collected from 4 independent studies. Each phylogenetic family was assigned a rank according to the relative abundance of mapped reads placed in the family in any given study; and its average rank calculated from the ranks in the 4 studies. Of the 511 families represented in all 4 datasets, the 25 of highest average rank are listed in the table. Families in colored font were found to be prominently represented in our own 16S rRNA profiling studies of the mouse airway microbiome (Section 2.2).

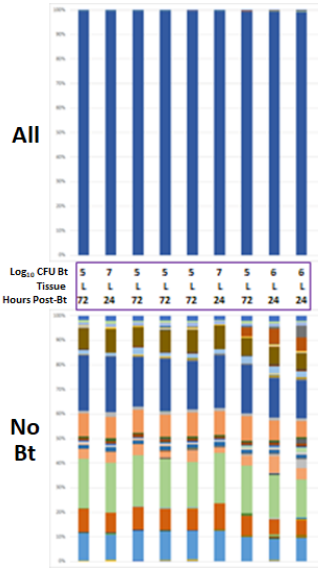

Figure 2. 16S rRNA Profiles of Bacteria in Lungs from Bt-Infected Mice. Bt was administered to the airway *via* OPA, in doses ranging from $2x10^3$ to $2x10^7$ CFU. At pre-defined times of 1-5d post-challenge, lungs were collected, homogenized, and 16S rRNA profiled. The top panel ("All") shows that the bacteria detected in the lungs were virtually all Bt (Burkholderiaceae family). Having removed the Bt-derived reads from the datasets, the bottom panel ("No Bt") shows that the minority families (Oxalobacteraceae, Neisseriaceae, Enterobacteriaceae, Comamonadaceae, Lactobacillaceae, Alcaligenaceae, Bacillaceae) are represented in relative ratios that vary little with Bt dose or collection time.

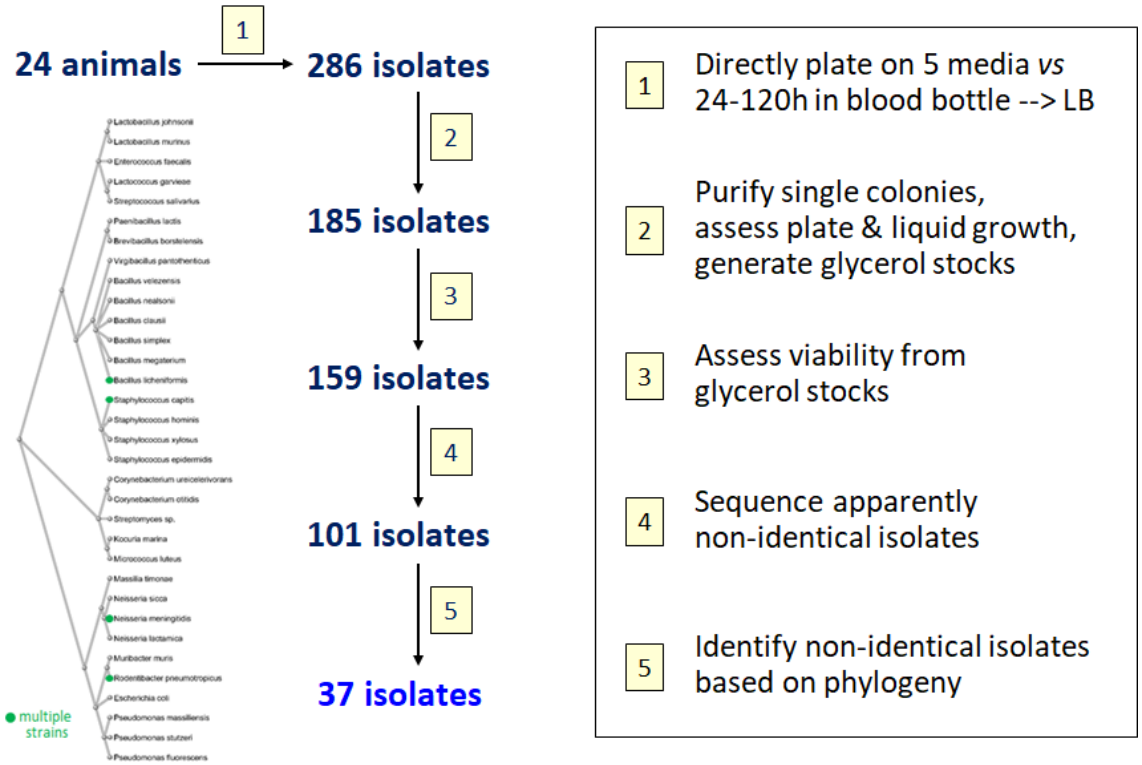

Figure 3. Overview of Culturomic Profiling of Mouse Airway Microbiome. Flowchart illustrates the process by which 37 genetically-distinct airway microbiome constituents were isolated, propagated

in culture, and identified *via* NGS. Phylogenetic tree shows placements based on NGS results; green dots indicate that multiple genetically-distinct isolates were called as the same species.

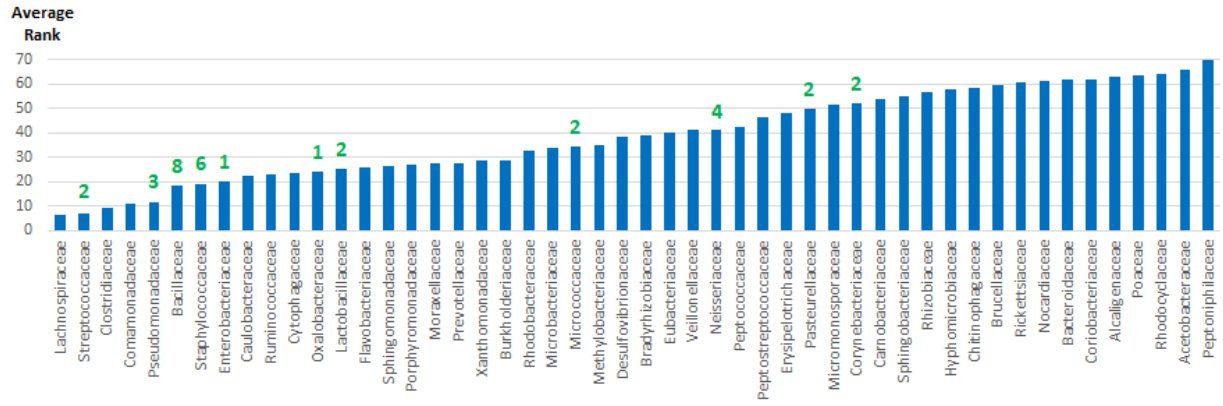

Figure 4. Mouse Airway Microbiome Constituents Recovered into Culture Predominantly Belong to Phylogenetic Families Robustly Represented in the Mouse Airway. Blue bars indicate average ranking of families based on representation in 16S rRNA profiles of the mouse airway microbiome (Section 2.1). Green numbers indicate the number of airway isolates that belong to each family. Of the 37 isolates, 4 do not belong to the 25 families shown here: 2 Paenibacillaceae (ave rank: 94), 1 Actinomycetaceae (ave rank:138), and 1 Enterococcaceae (ave rank: 79).

3. AIM 2: ENHANCE THE AIRWAY MICROBIOME USING PREBIOTICS AND PROBIOTICS.

We sought to determine whether any of the 37 genetically-distinct mouse airway microbiome constituents recovered through our culturomic profiling effort (Section 2.3) might serve as airway probiotics that protect against respiratory Bt infection. Additionally, we sought to identify nutrients that could confer an advantage to these candidate probiotics (CPs) in competing against Bt, with the idea that these could serve as preparative measures (feeding CPs prior to re-introduction into the airway), prebiotics (feeding CP equivalents *in situ*), and/or components of synbiotics (feeding CPs upon re-introduction into the airway). However, comprehensive evaluation of all 37 CPs wasn't feasible given the project's time and budget constraints. Therefore, we carried out a series of analyses to inform prioritization of CPs for evaluation as probiotics and development of prebiotics/synbiotics. First, we scanned the CP genome sequence assemblies (Section 2.3) for features that could provide the CPs with a competitive advantage over Bt (Section 3.1). Then, we assessed the CPs for ability to inhibit growth of Bt on LB agar (Section 3.2). Based on the results from these two efforts, we prioritized the CPs for evaluation of their ability to re-colonize the mouse airway. As it turned out, we were able to evaluate all CPs for colonization ability, with the exception of 7 CPs that did not grow robustly enough in culture to support evaluation (Section 3.3). The results from these studies (summarized in **Table 3**) informed prioritization of CPs for evaluation as probiotics (Section 3.4), as well as for growth requirement profiling to support development of prebiotics/synbiotics (Section 3.5).

It should be noted that in some of these studies we included a few strains that were not recovered from the mouse airway:

- 3 Bt mutants (*bsaS*::Tn, *bimA*::Tn, and *tssK5*::Tn) in which a gene encoding a structure required for virulence [type III secretion system component, actin-based motility protein, and type VI secretion system (T6SS) component, respectively] is disrupted. We had previously confirmed that all 3 mutants show little to no virulence *in vitro*, as evident from plaque formation assay results; and others had shown that equivalent mutants show little to no virulence in mice [22-25]. Our hypothesis was that these Bt mutants might successfully compete against wild-type Bt (being otherwise isogenic) and therefore serve as airway probiotics, protecting mice against respiratory (wild-type) Bt infection. We refer to these Bt mutants as CP15, CP11, and CP16, respectively.
- 2 *Bacillus subtilis* strains (3610 and 168) that are commonly used as models for *B. subtilis*, *Bacillus*, and indeed Gram-positive bacteria. We had noticed that several of the CPs were *Bacillus* strains, or from related genuses (*Paenibacillus*, *Brevibacillus*, *Virgibacillus*, and *Lactobacillus*), and wondered whether *B. subtilis* might share potential as an airway probiotic. We refer to these *B. subtilis* strains as CP42 and CP43, respectively.

3.1. Predicted Competitive Advantages of CPs *vs* Bt Based on Genome Annotation.

Each CP genome sequence assembly (Section 2.3) was scanned for features that could indicate a competitive advantage over Bt. The results from these analyses are summarized in **Table 3** (columns 4-8).

Auxotrophies for amino acids, cofactors, vitamins, and quinones were predicted using a KBase [26] software tool, and the auxotrophy profile of each CP was compared to that of Bt in order to identify

potential competitive advantages (*i.e.*, CP prototrophy + Bt auxotrophy for a given growth requirement). A qualitative score was assigned to each CP based on the number of potential competitive advantages identified (**Table 3**, column 4).

Ability to produce compounds that could confer a competitive advantage *vs* Bt was predicted using BAGEL4 [27] (bacteriocins), BACTIBASE [28] (bacteriocins), and antiSMASH [29] (antibiotics and siderophores). A qualitative score was assigned to each CP based on the number of compound-production features identified and the levels of confidence in these calls (+++ = >10 compounds; ++ = 5-10 compounds; + = <5 compounds; +/- = <5 compounds with little supporting annotation) (**Table 3**, column 5).

Ability to produce an anti-bacterial T6SS was predicted on the basis of BLAST-mediated identification of gene clusters that together encode all required components of T6SS, using genome annotation tools available through PATRIC [30,31]. Genes potentially encoding T6SS-delivered effector proteins were identified through search of sequences located between *vgrG* and *icmF* genes in and near the T6SS gene clusters, in accordance with a previously established approach [32]. A qualitative score was assigned to each Gram-negative CP (Gram-positive bacteria do not produce T6SS) based on the number of T6SS gene clusters and effector genes identified (+++ = >1 T6SS gene cluster with >1 effector gene; ++ = 1 T6SS gene cluster with >1 effector gene; + = 1 T6SS gene cluster with 1 effector gene; +/- = 1 T6SS gene cluster lacking an effector gene) (**Table 3**, column 6).

Ability to produce a contact-dependent growth inhibition (CDI) system was predicted on the basis of sequence motifs identified through use of the MEME Suite [33], MAST [34], and PATRIC [30,31]. A qualitative score was assigned to each Gram-negative CP (Gram-positive bacteria do not produce CDI systems) based on the number of sequence motifs identified (**Table 3**, column 7).

Ability to produce a wall-associated protein A (WapA) anti-bacterial weapon was predicted on the basis of sequence motifs identified through use of RASTtk [31] analysis of inferred translation products. A qualitative score was assigned to each Gram-positive CP (Gram-negative bacteria do not produce WapA) based on the number of characteristic motifs (up to 10 in total) clustered together on the chromosome (+++ = 10 motifs; + = 5-7 motifs) (**Table 3**, column 8).

3.2. Assessment of CPs for Ability to Inhibit Bt Growth *In Vitro*.

Each CP was assessed for ability to inhibit Bt growth on LB agar, using a halo assay approach. In these experiments, the CPs and Bt were grown in individual liquid LB cultures at 37°C with shaking (250 rpm) for 16 h. The Bt culture was diluted with LB, then spread as a lawn on LB agar. Once the Bt lawn had dried, the CPs were spotted on the lawn, and the plate incubated at 37°C for 1 d. CP-mediated inhibition of Bt growth (as evident in a clear halo in the Bt lawn surrounding the spotted CP) was assigned a qualitative score (**Table 3**, column 9).

It should be noted that, following this effort, our collaborators at UC-B and GIT carried out much more sophisticated analyses of CP-mediated inhibition of Bt *in vitro*.

At UC-B, the focus was assessment of CP-mediated inhibition of Bt in liquid co-cultures, initially using LB as the culture medium but ultimately transitioning to a synthetic sputum (sSputum) medium meant to more closely approximate the chemical composition of airway secretions. The sSputum recipe (25mM D-glucose + 56mM L-lactate + AA mix + 10mM CaCl2 + 4mM MgCl2 + 6 mM

FeSO4, buffered to pH 7) was based on the composition of sputum from cystic fibrosis patients, as assessed through nuclear magnetic resonance spectroscopy [35], with minor alterations to chloride and sodium concentrations in order to bring them into accordance with the normal range for sputum from healthy patients. Each CP was incubated in sSputum at 37°C with shaking (250 rpm) for 1-2 d, combined with Bt in sSputum at ratios ranging from 1:10,000 to 1000:1 (CP:Bt), and the co-cultures incubated at 37°C with shaking (250 rpm) for 1 d. Finally, dilutions of the co-cultures were plated on LB + carbenicillin agar and, after incubation at 37°C for 1-2 d, the Bt CFU enumerated in order to quantify CP-mediated killing of Bt in co-culture. Perhaps the most striking finding from these studies is that while CP8 (*Bacillus velezensis*) and CP19 (*Brevibacillus borstelensis*) both individually kill Bt in co-culture (absolute IC50 values of 1.73700 and 0.00744, respectively), the combination kills far more efficiently (absolute IC50 value of <0.00003) (**Figure 5**), indicating a synergistic effect.

At GIT, the focus was identification of secondary metabolites produced by CPs and Bt in co-culture in liquid and on solid media (tryptic soy broth and agar, respectively), as assessed through mass spectrometry (LC-MS and MALDI-IMS, respectively). Example results from this work are shown in **Figure 6**. In this case, CP8 was found to induce production of capistruins (lasso peptide antibiotics that inhibit RNA polymerase) [36] by Bt and, in turn, Bt induced production of bacillaene and dihydrobacillaene (highly-conjugated linear polyene antibiotics that disrupt protein synthesis) [37] by CP8.

3.3. Assessment of CPs for Ability to Re-Colonize the Mouse Airway.

Each CPs was assessed for ability to re-colonize the mouse airway, using a new protocol established in the course of this project. In these experiments, the CP was cultured in LB at 37°C with shaking (250 rpm) for 16 h, recovered through centrifugation, resuspended in PBS, and diluted to an OD_{600} corresponding to $3.3x10^7$ CFU/ml (based on prior determination of OD_{600} --> CFU plating efficiency). 30 µl of this dosing material (corresponding to 10^6 CFU) were administered to the airway *via* OPA (3 mice *per* CP). After 7 d (colonization period), airway and liver tissues were collected, homogenized, and diluted in PBS. 100 µl aliquots of homogenate dilutions were used to inoculate LB agar, the plates were incubated at 37°C, and at 1-5 d post-inoculation the CFU on each plate were enumerated. A qualitative score was assigned to each CP based on: 1) The average number of CFU recovered from the airway; 2) The consistency with which CFU were recovered; and 3) Failure to recover CFU from the liver (indicating lack of dissemination); multiple scores indicates that the CP was evaluated in multiple experiments (**Table 3**, column 11).

We found that of the 31 CPs tested, only 8 could be consistently recovered from the mouse airway after the 7-d colonization period, and 7 of these belonged to the Firmicutes phylum (**Figure 7**). In fact, all 6 of the CPs that colonized most robustly belonged to *Bacillus* or a closely related genus (**Figure 8**). However, not all CPs in *Bacillus* or a closely related genus were able to colonize: We found that 4 CPs originally recovered from the mouse airway and belonging to *Bacillus* or a closely related genus were unable to re-colonize the airway, as were 2 *B. subtilis* strains included for comparison. Additionally, *Bacillus* CPs did not segregate with phylogenetic cluster as a function of colonizing ability (**Figure 9**). Taken together, these results indicate that ability to re-colonize the mouse airway is a trait predominantly found in, but not shared amongst all, *Bacillus* CPs; and that this trait is not restricted to a distinct phylogenetic cluster within *Bacillus*.

Given that *Bacillus* and closely related genuses are comprised of spore-forming bacteria, we wondered whether CPs belonging to these genuses were scored as colonizers simply because they were able to

persist as spores in the airway for 7 d. To address this question, we used phase-contrast microscopy to examine the CP dosing material administered to mice as well as the airway tissues collected after the 7-d colonization period. Representative results from this experiment are shown in **Figure 10**. We found that the dosing material was predominantly comprised of vegetative cells (sometimes in long chains), as expected; and that colonizing CPs detected in airway homogenates were in vegetative form as well. These results suggest that colonizing CPs do not simply persist in the airway as spores, but instead generally assume vegetative form in the airway.

We should note that none of the CPs tested for ability to re-colonize the airway were recovered from the liver after the 7-d colonization period, with the exception of a Bt mutant (CP11 = *bimA*::Tn) that unexpectedly caused lethal infection, contrary to previous observations [34,35]. These results suggest that the tested CPs (aside from CP11) do not disseminate from the airway.

3.4. Evaluation of *Bacillus* CPs as Airway Probiotics.

We hypothesized that ability to re-colonize the airway would be a baseline requirement for, or at least an important contributing factor to, CP-mediated protection against respiratory Bt infection. Therefore, we initially assessed only the colonizing *Bacillus* CPs for anti-infective activity *in vivo*. In these experiments, CP dosing material was prepared, and 10^6 CFU administered *via* OPA, as for the colonization studies (Section 3.3). At 3 d or 7 d post-treatment, the previously-determined minium lethal dose (MLD) of Bt ($3x10^4$ – $5x10^5$ CFU) was administered *via* OPA. The rationale for the 3-d treatment period was that it would be enough time to allow for settling of immediate host responses to the CP, yet not enough to risk clearance of most CP bacteria from the airway, prior to Bt challenge. The rationale for the 7-d treatment period was that it would better highlight long-term protective effects, which we expected to require CP colonization. At 3 d post-challenge (corresponding to 6 d or 10 d post-treatment), airway and liver tissues were collected, homogenized, and diluted in PBS. 100 µl aliquots of homogenate dilutions were used to inoculate LB agar, the plates were incubated at 37°C, and at 1-5 d post-inoculation the CFU on each plate were enumerated. Results from a representative experiment are shown in **Figure 11**. We found that in the Bt-infected mice, the CPs could be detected in the airway at 6 d post-treatment (upper-left panel) but not at 10 d post-treatment (lower-left panel). The CPs were not detected at all in the liver (right panels), consistent with the results from our colonization studies (Section 3.3) and strongly suggesting that the CPs do not disseminate to other tissues from the airway. Treatment with CP8 had no noticeable effect on Bt loads in the airway or liver, regardless of treatment period. In contrast, CP13 treatment at 3 d prior to Bt challenge resulted in reduced Bt loads in both the airway and liver, the former effect reaching statistical significance (unpaired Student's *t*-test *p*-value = 0.0298). However, CP13 treatment at 7 d prior to Bt challenge did not markedly reduce Bt loads in the airway or liver. Taken together, these results indicated that CP8 treatment does not protect mice against respiratory Bt infection, whereas CP13 can provide some protection when the treatment is administered at 3 d (but not 7 d) prior to Bt challenge.

In a more elaborate follow-on experiment, we assessed all of the colonizing *Bacillus* CPs for ability to protect against respiratory Bt infection (as evident in reduced loads of Bt in the liver) when CP treatment preceded Bt challenge by 3 d. CP and Bt dosing, liver collection at 3 d post-challenge, and enumeration of CFU in liver were carried out as described above. Additionally, we monitored body weight as a metric for general health of the mice. The results from this experiment are shown in **Figure 12**. We found that the most of the colonizing *Bacillus* CPs provided protection against respiratory Bt infection (as evident from markedly reduced Bt loads in liver, as well as rebound from

initial weight loss) when administered 3 d prior to Bt challenge. The notable exception was CP8, which provided little to no protection (CP28 appeared to provide protection inconsistently).

In light of their protective effects with regard to reducing Bt loads in airway and liver, and to halting weight loss following Bt challenge, it seemed possible that the CPs might also enable mice to survive an otherwise lethal Bt infection. To address this question, we carried out a series of experiments in which colonizing and non-colonizing *Bacillus* CPs were individually used to treat mice (5 *per* group) at 3 d, 5 d, or 7 d prior to challenge with Bt at the MLD, and mortality monitored for 10 d post-challenge. The results from these experiments are summarized in **Figure 13**. Consistent with our previous observations, we found that most of the *Bacillus* CPs provided robust protection against respiratory Bt infection (evident in ≥75% survival, whereas untreated infection resulted in ≤20% survival) when administered 3 d prior to Bt challenge (top row). The exceptions were CP8, which failed to protect (20% survival); and CP18 and *B. subtilis* (CP42), which provided weak protection (45-55% survival). CP treatment at 5 d prior to Bt challenge generally resulted in weaker protection (middle row). The most notable exceptions were CP17 and CP19 (≥90% survival), followed by CP21, CP27, and CP28 (50-70% survival). Finally, CP treatment at 7 d prior to Bt challenge did not provide protection, with CP19 being the only exception (~60% survival) (bottom row). Contrary to our expectation, ability to protect did not closely correlate with ability to colonize; however, it should be noted that the only protection observed when treatment preceded Bt challenge by 7 d was achieved by CP19, which robustly colonizes the mouse airway (Section 3.3). In summary, our results indicate that most *Bacillus* CPs are capable of providing protection against respiratory Bt infection when administered 3 d prior to Bt challenge, but degree of protection decreases as the interval between CP treatment and Bt challenge increases, with only CP19 capable of protecting when administered 7 d prior to Bt challenge.

3.5. Identification of Nutrients that Could Serve as Airway Prebiotics.

We took two different approaches to identifying candidate airway prebiotics:

- Comparative analysis of CP *vs* Bt growth requirements *in vitro*, in order to identify nutrients that could favor the CP in its competition with Bt *in vivo*.
- Assessment of nutrients for ability to induce or enhance CP-mediated inhibition of Bt *in vitro*, with the idea that similar effects could be achieved *in vivo*.

Both approaches depended on use of Biolog Phenotype Microarrays (PMs) [38]: 96-well microtiter plates in which every well contains a base medium supplemented with a different essential nutrient, such that 96 different growth media can be tested in parallel for ability to support culture of a given microbe (in our case, a CP or Bt). The PMs are placed in an automated instrument (OmniLog) that maintains temperature while periodically measuring metabolic activity in each well (through colorimetric detection of cellular respiration).

In the first approach, a subset of the *Bacillus* CPs (CP8, CP13, CP18, CP19, and CP26) were cultured in PM01 and PM2A (both varying carbon source). CP8, CP13, CP17, and CP19 were also cultured in PM3B (varying nitrogen source). For comparison, Bt was cultured in PM01, PM2A, and PM3B. The OmniLog maintained the inoculated PMs at 33^{o}C, and took metabolic activity readings every 15 min for 2 d. Results from a representative experiment are shown in **Figure 14**. We found that 7 different carbon sources favored CP8 metabolic activity over Bt metabolic activity by ≥2-fold (left panels, green highlights), whereas only 1 favored CP19 over Bt (right panels, green highlights). There was no overlap in these CP-favoring carbon sources, which suggests that it will be difficult or impossible to identify a universal prebiotic that provides all CPs of interest a competitive advantage over Bt. On the other hand, the carbon and nitrogen sources observed to provide individual CPs of interest a competitive advantage over Bt *in vitro* can now be evaluated as candidate prebiotics (individually and/or in combination) and synbiotics (administering them together with the CPs that they favor) *in vivo*.

In the second approach, CP8 and CP19 were individually cultured in PM01 and PM2A at 37^{o}C for 2 d; wells supporting robust metabolic activity [peak value ≥50 arbitrary units (AU)] were used as the CP source for spotting onto a lawn of Bt (spread using a 0.7% agar overlay); and CP-mediated inhibition of Bt (as evident in a clear halo surrounding the CP spot) was scored after 16 h - 2 d incubaion at 37^{o}C. Results from a representative experiment are shown in **Figure 15**. Consistent with previous observations (Section 3.2), we found that CP8 generally inhibited Bt regardless of culture conditions. However, we observed enhanced inhibition when CP8 was provided D-fructose (left panel, 4) or glycerol (right panel, 7) as the carbon source. In contrast, CP19 was not observed to inhibit Bt under any culture condition. These results suggest that it may be easier to identify nutrients that enhance (rather than induce) CP-mediated inhibition of Bt *in vitro*.

Candidate Probiotic	Isolate/Mutant	Species	Predicted Auxotrophies	Predicted Compounds	Predicted T6SS	Predicted CDI	Predicted WapA	Anti-Bt on LB	Testing Priority	Colonization Score	Notes
CP8	20sb3L1	Bacillus velezensis	++	+++	NA	NA	+++	+++	1	++ +++ ++	
CP3	9K1	Shigella boydii	+	+	++	+++	NA	+	1	+	
CP4	12b2L1	Pseudomonas moraviensis	+++	++	+++	-	NA	+	1	-	
CP7	17spA3	Pseudomonas stutzeri	++	+	++	-	NA	+	1	-	
CP13	15aJ1	Bacillus licheniformis	+	+++	NA	NA	-	+	1	+++ +++ +++	
CP26	17ab3L1	Bacillus licheniformis	++	ND	NA	NA	ND	ND	ND	+++ ++ +++	
CP6	15sb3L2	Staphylococcus hominis	+	+	NA	NA	-	+	1	+	
CP1	2K1D-1	Neisseria subflava	+++	+/-	++	+	NA	-	1	+/-	
CP2	7J1	Rodentibacter myodis	+	+/-	++	+++	NA	-	1	+/-	
CP24	12b2J3	Pseudomonas massiliensis	++	+	++	+	NA	-	1	-	
CP20	19aL1	Bacillus clausii	+	++	NA	NA	+++	-	2	++ ++ ++	
CP9	24apL6	Neisseria lactamica	+++	+/-	++	-	NA	-	2	-	
CP34	17spA1	Massilia timonae	+	+/-	++	-	NA	ND	2		Difficult to grow
CP28	18apH1	Bacillus nealsonii	++	+/-	NA	NA	+	-	2	+++ +++ +	
CP18	8b1L1	Bacillus simplex	+++	++	NA	NA	-	-	2	- - +/-	
CP21	22aJ1	Paenibacillus lactis	+++	++	NA	NA	-	-	2	- - +/- +/-	
CP36	24apL5	Neisseria sicca	+++	ND	++	ND	NA	ND	2		Difficult to grow
CP17	17apH1	Bacillus megaterium	++	++	NA	NA	-	-	2	+++ +/- - -	
CP19	15ab1L1	Brevibacillus borstelensis	++	++	NA	NA	-	-	2	++ +++ +++	
CP25	17ab2L1	Staphylococcus epidermidis	++	++	NA	NA	-	-	2	-	
CP14	2K1B-1	Streptomyces sp.	+	+++	NA	NA	-	-	2	+/-	
CP22	2K2-1	Corynebacterium otitidis	+++	+	NA	NA	-	-	2	-	
CP23/37	19apA2	Kocuria marina	+++	+	NA	NA	-	-	2		Difficult to grow
CP5	13A1	Staphylococcus capitis	+	++	NA	NA	-	-	2	-	
CP27	23aA1	Virgibacillus pantothenticus	+	++	NA	NA	-	-	3	- - +	
CP33	19apA1	Micrococcus luteus	++	+	NA	NA	-	-	3		Difficult to grow
CP30	7A1	Staphylococcus xylosus	+	++	NA	NA	-	-	3	-	
CP38	6A1	Lactobacillus murinus	+/-	++	NA	NA	-	-	3		Difficult to grow
CP29/39	5A1-1	Corynebacterium ureicelerivorans	++	+/-	NA	NA	-	-	3	-	
CP31	24apL3	Staphylococcus salivarius	+	+/-	NA	NA	-	-	3		Difficult to grow
CP15	bsaS::Tn	Burkholderia thailandensis	NA	ND	+++	ND	NA	NA	3	+/-	
CP11	bimA::Tn	Burkholderia thailandensis	NA	ND	+++	ND	NA	NA	3	-	Lethal
CP16	tssK5::Tn	Burkholderia thailandensis	NA	ND	+++	ND	NA	NA	3	-	
CP32/40	9b1A1-2	Lactococcus garvieae	-	+	NA	NA	-	-	4	-	
CP41	2K1	Lactobacillus johnsonii	-	+/-	NA	NA	-	-	4		Difficult to grow
CP35	11H1	Enterococcus faecalis	-	+/-	NA	NA	-	-	4	-	
CP42	3610	Bacillus subtilis	ND	ND	NA	NA	ND	ND	ND	+/- - -	
CP43	168	Bacillus subtilis	ND	ND	NA	NA	ND	ND	ND	+/-	

Table 3. Results from Initial Characterization of CPs to Inform Prioritization for Further Study. NA = not applicable, ND = not done.

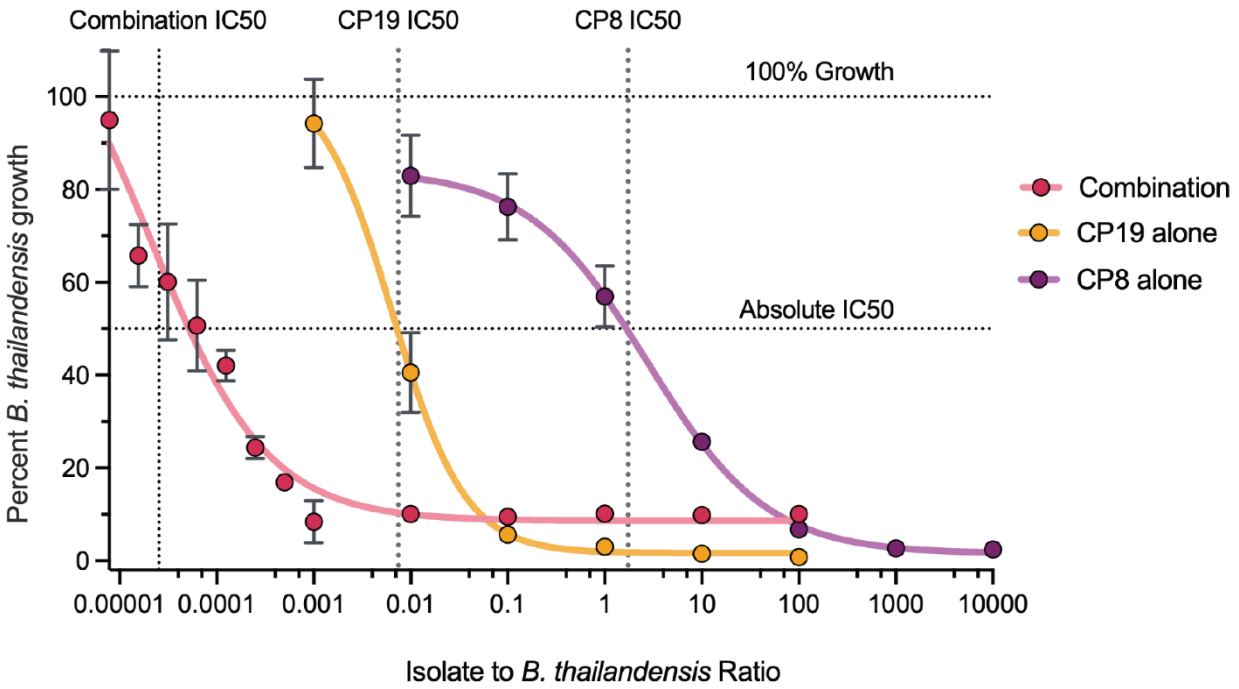

Figure 5. Synergistic Killing of Bt in sSputum Co-Culture by CP8 and CP19.

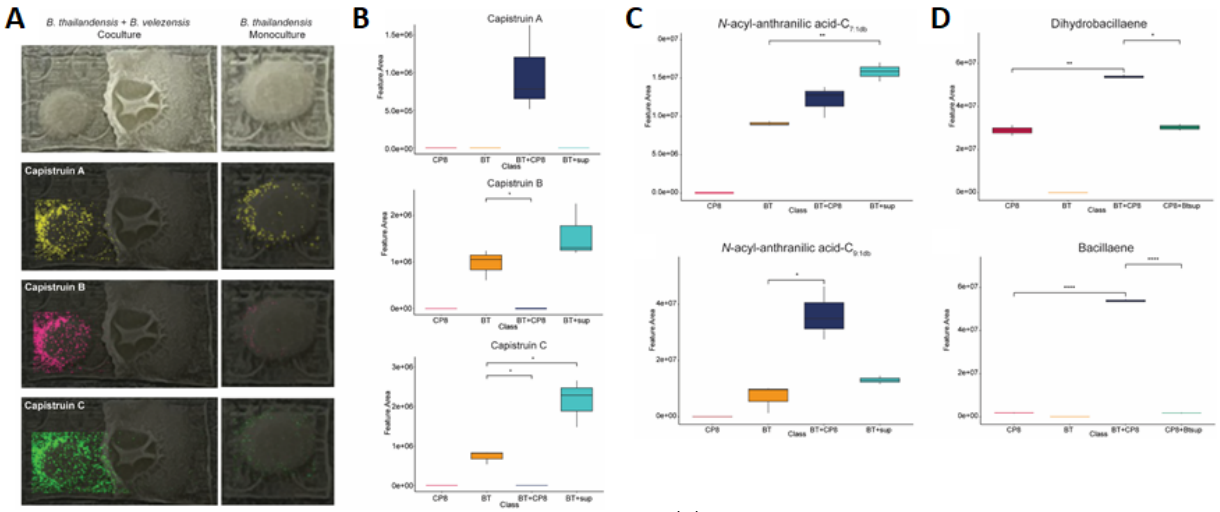

Figure 6. Antibiotics Produced by CP8 and Bt in TSB Co-Culture. **A.** MALDI-IMS images separately filtered for the [M+H] for each capistruin (m/z 2049.030, 1934.987, and 1787.919 for A, B, and C, respectively). **B.** Box plots of the relative intensity of each capistruin under the specified culture conditions, as measured using LC-MS. **C.** Box plots of the relative intensities of 2 n-acyl-anthranilic acids produced by Bt under the specified culture conditions, as measured using LC-MS. **D.** Box plots of the relative intensities of bacillaene compounds produced by CP8 under the specified culture conditions, as measured using LC-MS.

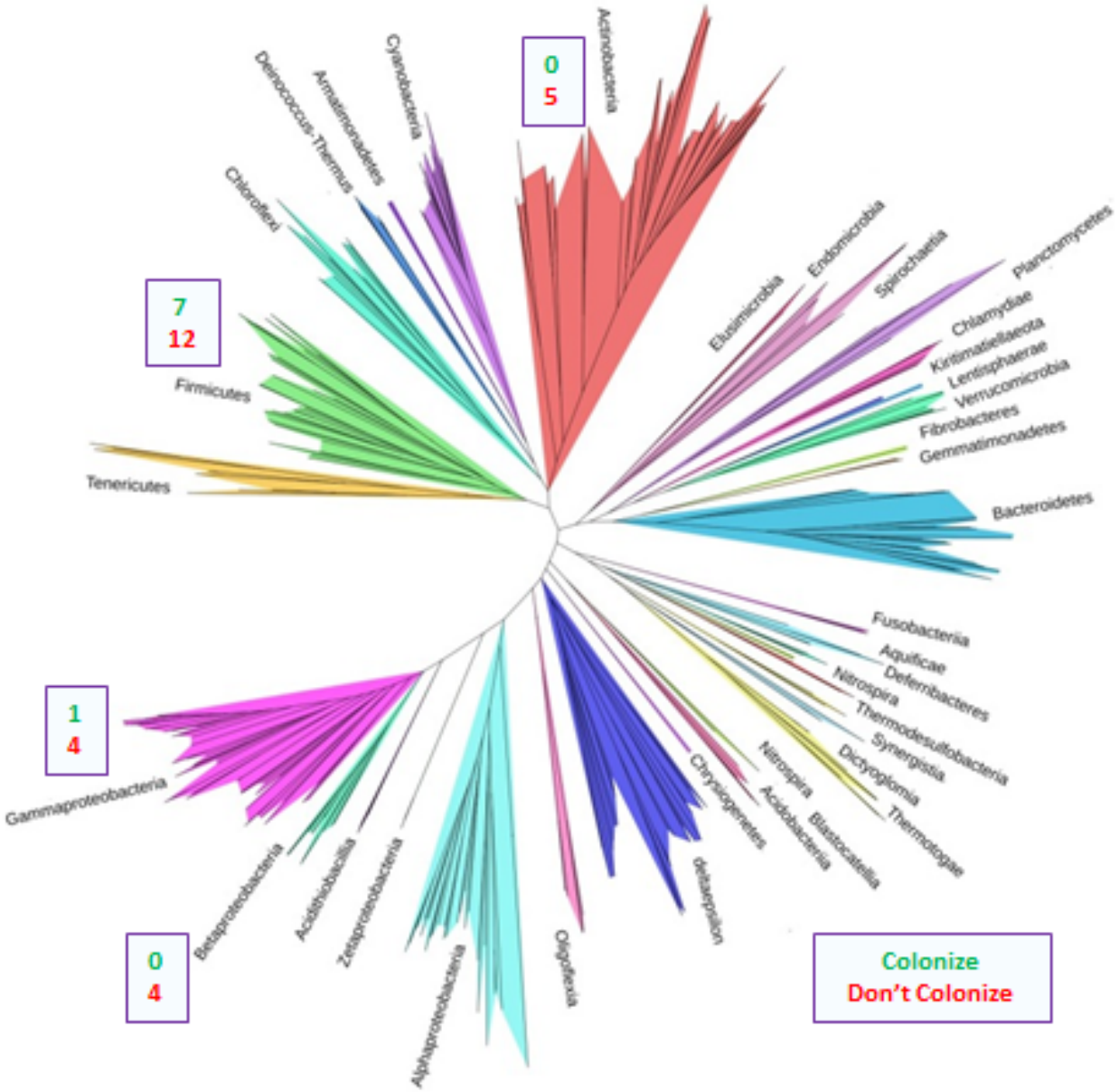

Figure 7. Phylogenetic Distribution of CPs Tested for Ability to Re-Colonize the Mouse Airway. Top numbers in green font indicate the number of CPs in the phylogenetic category that were able to re-colonize the mouse airway; bottom numbers in red font indicate the number that were unable to re-colonize. Phylogenetic tree from [39].

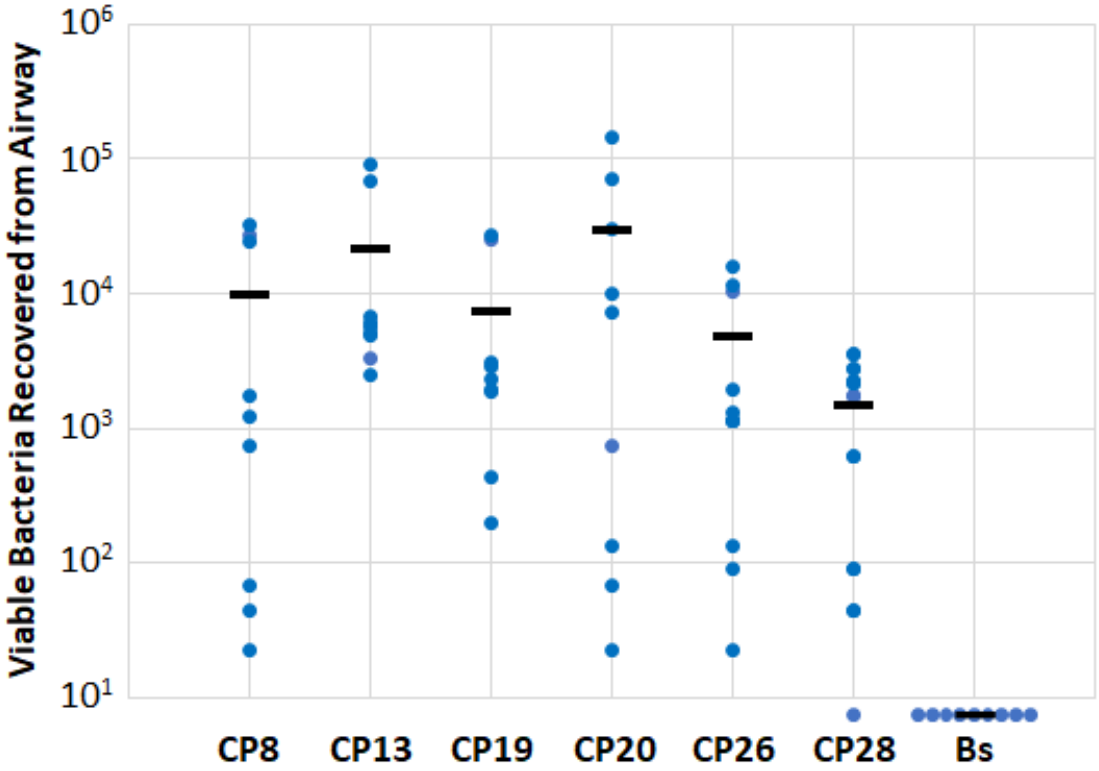

Figure 8. Degree and Consistency of Airway Re-Colonization by *Bacillus* CPs. For each CP, 10^6 CFU were administered to each of 3 mice *via* OPA and, after a 7-d colonization period, airway tissues were collected, homogenized, and used to inoculate LB agar for enumeration of CFU. Three independent experiments were carried out (total of 9 mice *per* CP). Blue data points indicate measured CFU, black bars indicate average CFU. Bs = *B. subtilis* strain 3610 (CP42).

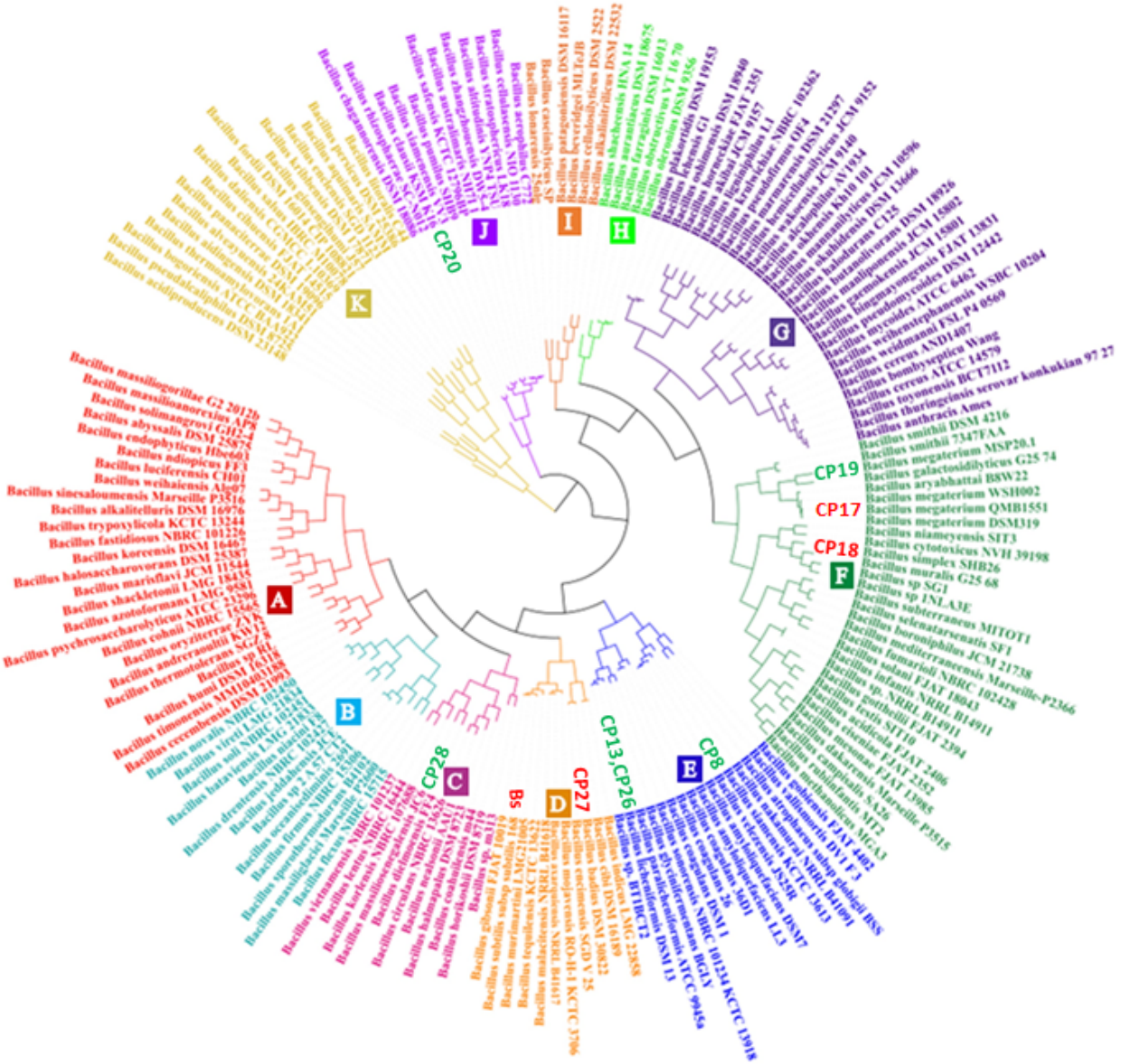

Figure 9. Phylogenetic Distribution of CPs That Belong to Genus *Bacillus*. Green font indicates that the CP was able to re-colonize the mouse airway, red font indicates that it was not. Phylogenetic tree from [40].

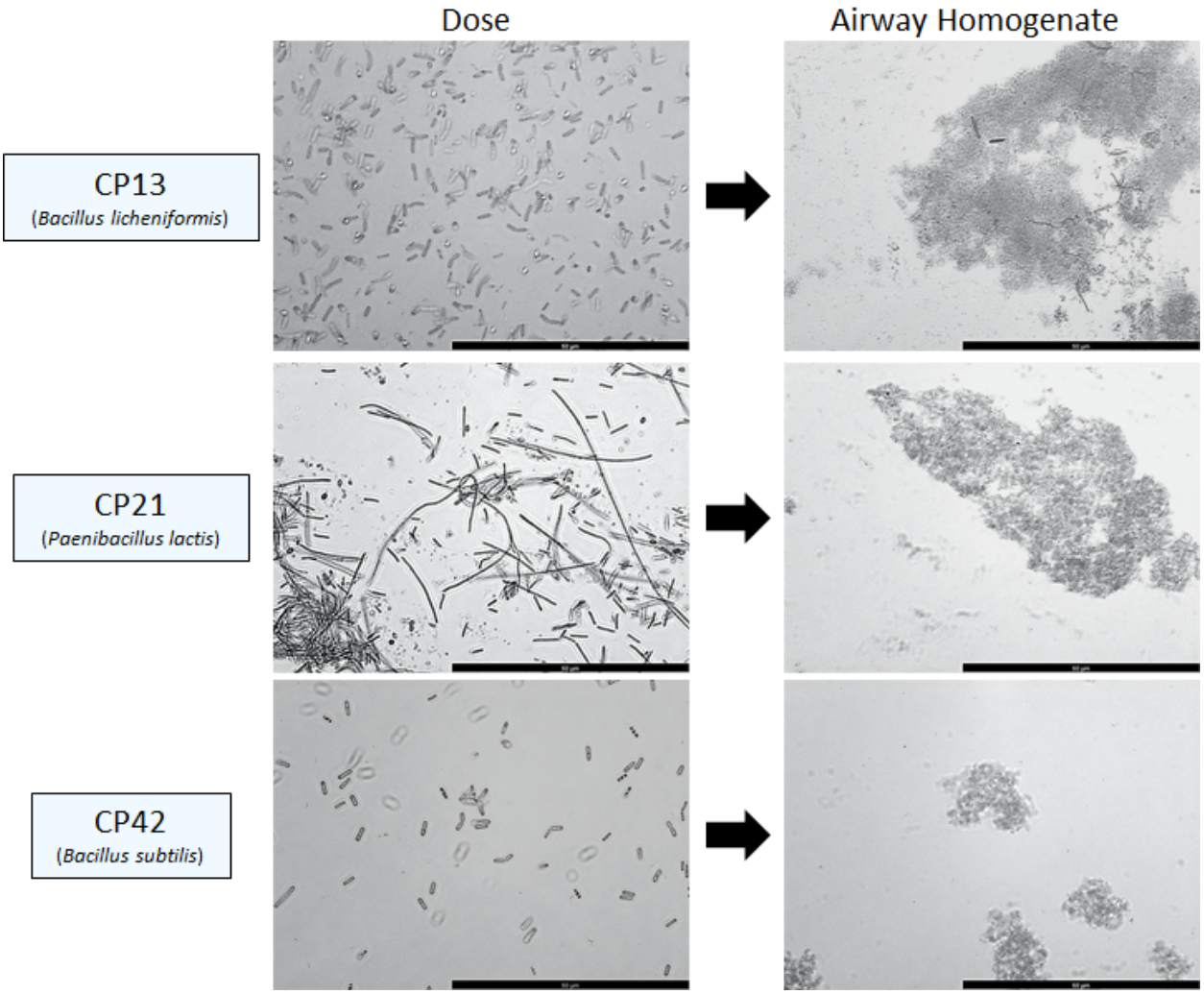

Figure 10. Phase-Contrast Microscopy Analysis of *Bacillus* CPs at Time of Dosing and After 7-d Colonization Period. Colonizing: CP13; non-colonizing: CP21 and CP42.

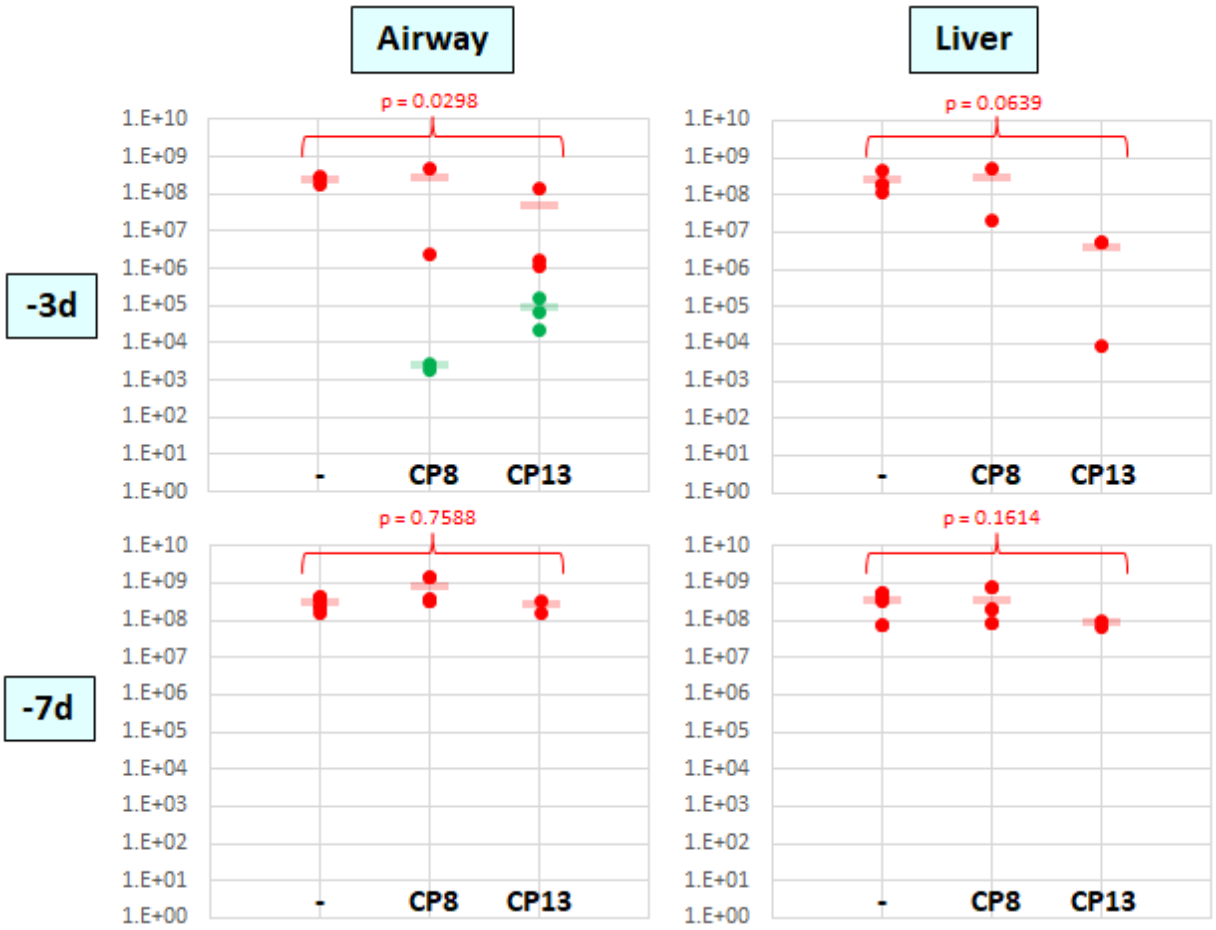

Figure 11. Bacterial Loads in Airway and Liver Tissues of Mice Treated with CPs and Then Challenged with Bt. 10^6 CFU of each CP were administered *via* OPA. At 3 d or 7 d post-treatment, $3.5x10^4$ CFU of Bt were administered *via* OPA. At 3 d post-challenge (corresponding to 6 d or 10 d post-treatment), airway and liver tissues were collected, homogenized, diluted, and plated on LB agar for enumeration of CP and Bt CFU. Data points indicate CP (green) and Bt (red) CFU measured (3 mice *per* group); bars indicate average CFU for each group. Unpaired Student's *t*-test *p*-values for comparision of Bt loads in untreated *vs* CP13-treated mice are shown.

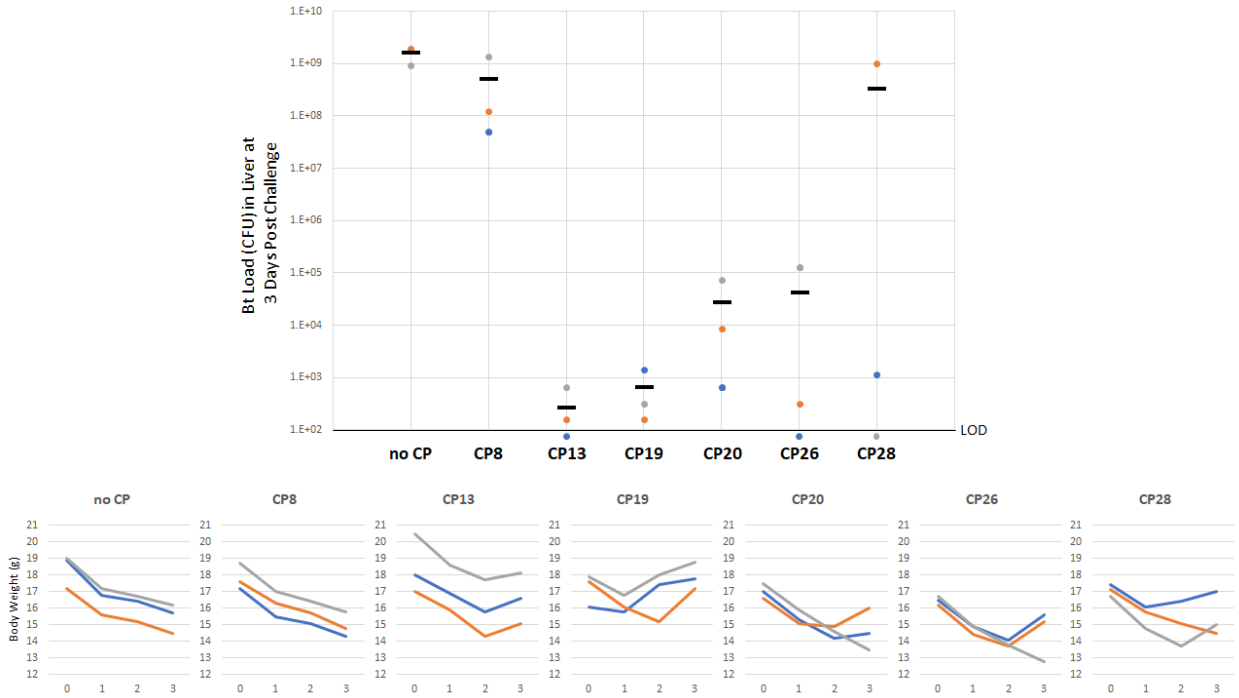

Figure 12. Bacterial Loads in Liver Tissues, and Body Weights, of Mice Treated with CPs and Then Challenged with Bt. 10^6 CFU of each CP were administered *via* OPA. At 3 d post-treatment, $3.5x10^4$ CFU of Bt were administered *via* OPA. At 3 d post-challenge (corresponding to 6 d post-treatment), liver tissues were collected, homogenized, diluted, and plated on LB agar for enumeration of Bt CFU. Body weights were measured daily. 3 mice *per* group. **Top:** Data points indicate Bt CFU measured; bars indicate average CFU for each group. **Bottom:** Line graphs of body weights starting at time of Bt challenge (0 d) and ending at time of tissue collection (3 d). Bt load (top) and body weights (bottom) from a given mouse are in the same color.

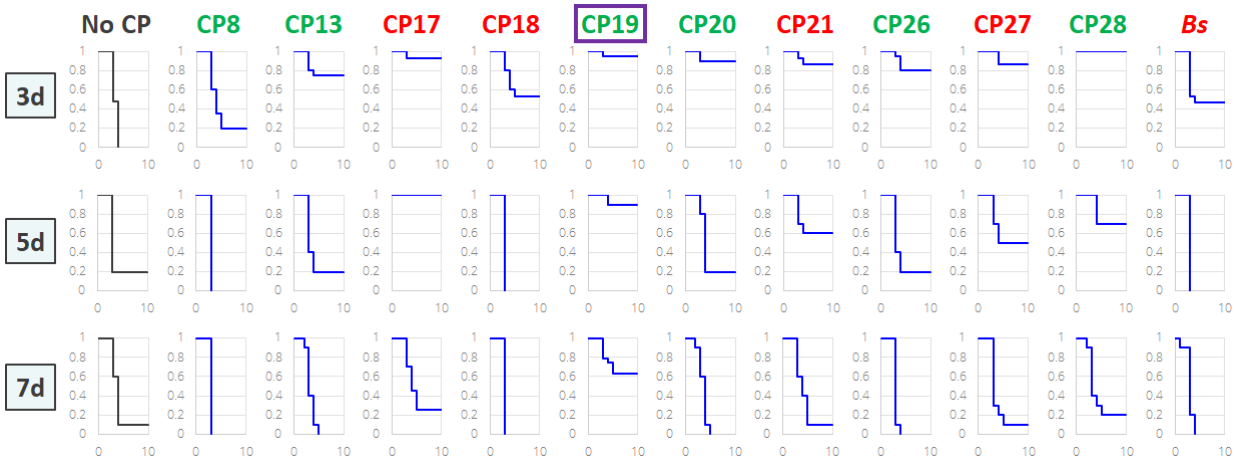

Figure 13. Survival Rates of Mice Treated with *Bacillus* CPs Prior to Bt Challenge at the MLD. 10^6 CFU of each CP were administered *via* OPA. At 3 d, 5 d, or 7 d post-treatment, Bt was administered at the MLD ($3x10^4$ – $5x10^5$ CFU) *via* OPA. Mortality was monitored for 10 d post-challenge; deaths were scored when mice were either found dead or euthanized at the humane endpoint (moribund and/or >20% weight loss). 5 mice *per* group; 1-5 studies (5-25 mice) *per* CP. Green font indicates colonizing CPs, red font indicates non-colonizing CPs. Bs = *B. subtilis* (CP42). Purple box highlights CP19, which displayed the most consistent protection.

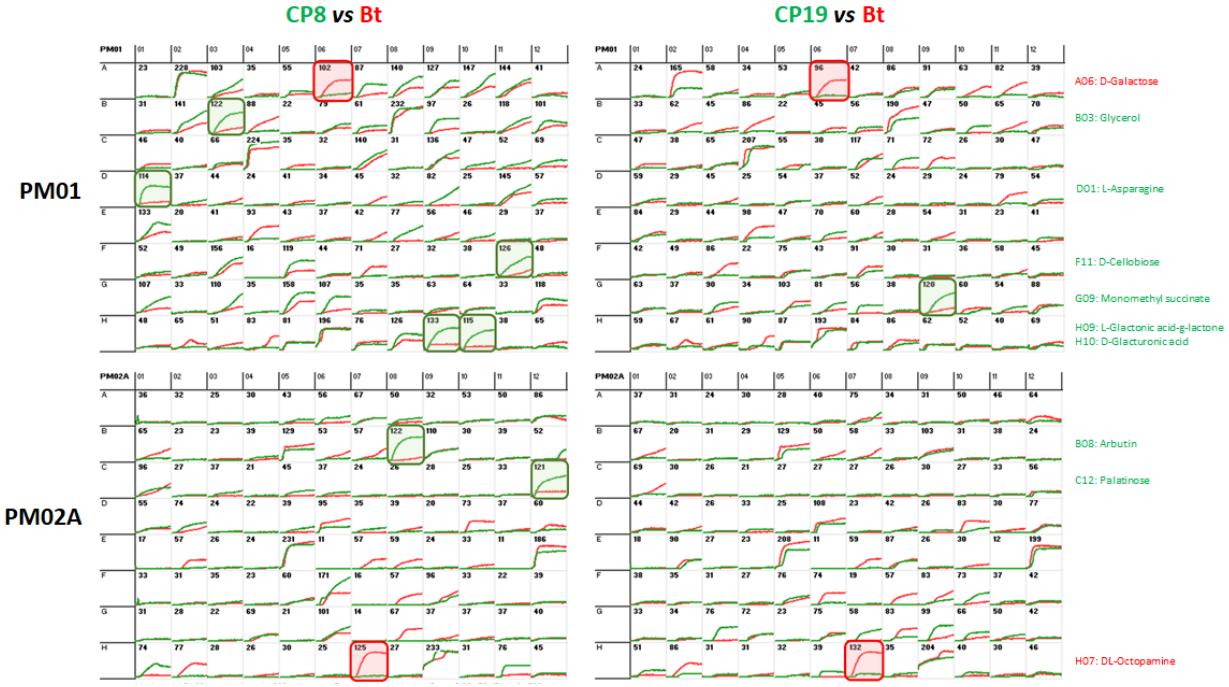

Figure 14. Comparative Growth Requirement Profiling of CPs *vs* Bt. CP8, CP19, or Bt was used to inoculate all wells within PM01 and PM2A (both varying carbon source). The PMs were maintained at 33°C, and metabolic activity in each well was measured every 15 min for 2 d. Green traces indicate CP metabolic activity, red traces indicate Bt metabolic activity (CP and Bt measurements were made in separate PMs and the results were superimposed); the black number in the upper-left corner of each graph indicates the peak value (AU) for metabolic activity in that well. Green highlighting indicates that CP metabolic activity exceeded Bt metabolic activity in that well by ≥2-fold; the carbon sources in these wells are listed to the right of the graphs, in green font. Red highlighting indicates that Bt metabolic activity exceeded CP metabolic activity in that well by ≥2-fold; the carbon sources in these wells are listed to the right of the graphs, in red font.

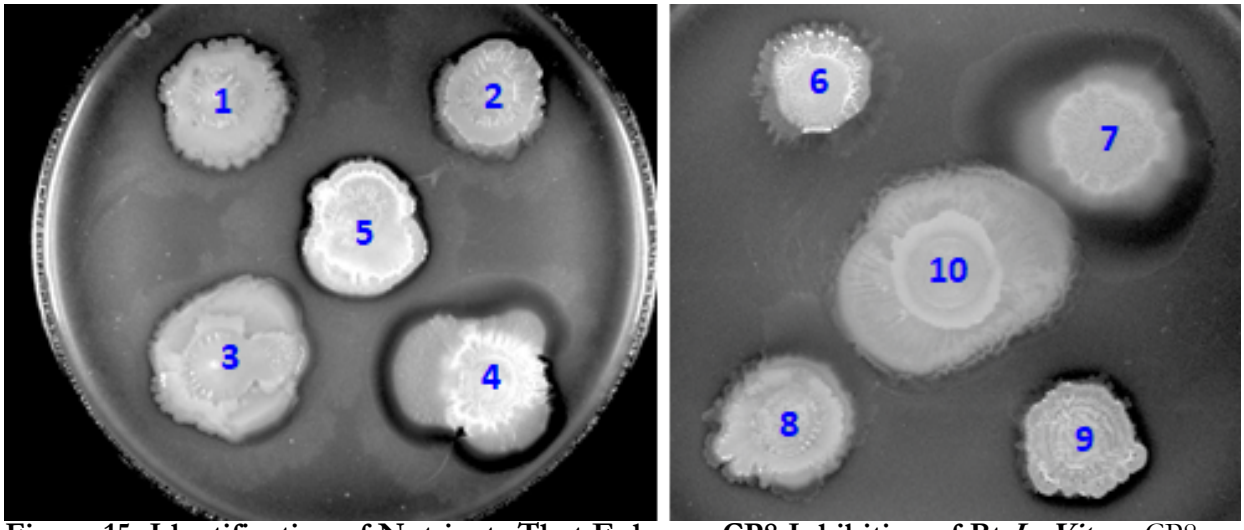

Figure 15. Identification of Nutrients That Enhance CP8 Inhibition of Bt *In Vitro*. CP8 was cultured in Biolog PM01 (varying carbon source) at 37°C for 2 d. A 3 µl aliquot from each well displaying robust metabolic activity (peak reading ≥50 AU) was spotted onto a Bt lawn (formed through agar overlay) on LB agar, and after incubation at 37°C for 16 h - 2 d the halos (indicating inhibition of Bt by the spotted CP) were scored. Carbon sources: L-glutamic acid (1); D-ribose (2); L-rhamnose (3); D-fructose (4); αD-glucose (5); D-gluconic acid (6); Glycerol (7); DL-α-glycerol phosphate (8); L-fucose (9); D-xylose (10).

4. CONCLUSIONS AND FUTURE DIRECTIONS.

Over the course of this project, we were able to make a number of significant technical advancements that together should serve as a strong foundation for further development, and eventual translation to clinical use, of airway probiotics, prebiotics, and synbiotics that provide protection against respiratory infection.

4.1. Conclusions.

- Respiratory Bt infection does not radically alter the core composition of the mouse airway microbiome.
    - We consider this conclusion to be preliminary, because our studies lacked high quality negative control data from uninfected mice (due to NGS library preparation problems). Future work should address this gap.
    - We found that the Oxalobacteraceae, Neisseriaceae, Enterobacteriaceae, Comamonadaceae, Lactobacillaceae, Alcaligenaceae, and Bacillaceae families are well represented in Bt-infected airways, as they are in uninfected airways.
- Most of the CPs bear genome features indicative of metabolic capabilities and weaponry that could provide competitive advantages against Bt.
    - CP/Bt prototrophy/auxotrophy pairings for amino acids, cofactors, vitamins, and quinones are quite common.
    - Many CPs are predicted to produce bacteriocins, antibiotics, T6SS, and CDI/WapA systems that could inhibit Bt.
- A number of CPs can inhibit Bt *in vitro*, with strength of inhibition varying with context.
    - CP8 showed the most robust and consistent inhibition of Bt across all contexts tested.
    - CP3, CP4, CP6, CP7, CP8, and CP13 inhibited Bt in halo assays on LB agar.
        - CP8-mediated inhibition was enhanced when D-fructose or glycerol was the sole carbon source.
        - CP19 did not display inhibition of Bt on LB agar even when cultured with a wide variety of carbon sources.
    - CP7, CP8, and CP19 inhibited Bt in sSputum liquid co-cultures.
        - CP8 and CP19 displayed synergistic inhibition.
- When co-cultured in/on tryptic soy broth/agar, CP8 and Bt induce each other to produce antibiotics.
    - CP8 induced Bt to produce capistruins A, B, and C.
    - Bt induced CP8 to produce bacillaene and dihydrobacillaene.
- CPs capable of re-colonizing the mouse airway predominantly belong to *Bacillus* or a closely related genus. However, not all *Bacillus* strains are capable of colonizing the mouse airway.
    - 7/8 colonizing CPs belong to Firmicutes.
    - 6/6 robustly colonizing CPs belong to *Bacillus* or *Brevibacillus*.
    - CPs belonging to *Bacillus* (2), *Paenibacillus* (1), and *Virgibacillus* (1) failed to re-colonize the mouse airway.
    - *B. subtilis* strains (2) failed to colonize the mouse airway.
- CPs re-colonize the mouse airway predominantly as vegetative cells, rather than as spores.

    - We consider this conclusion to be preliminary, because it is based on initial experiments that have not been replicated yet.
- Most *Bacillus* CPs can protect mice against respiratory infection when administered 3 d prior to Bt challenge; few can do so when administered 5 d prior; and only CP19 can do so when administered 7 d prior.
    - When administered 3 d prior, CP13, CP17, CP19, CP20, CP21, CP26, CP27, and CP28 protected robustly; CP18 and *B. subtilis* (CP42) protected weakly; and CP8 did not protect.
    - When administered 5 d prior, CP17 and CP19 protected robustly; and CP21, CP27, and CP28 protected weakly.
- Different carbon sources favored CP8 (7) or CP19 (1) metabolic activity over Bt metabolic activity by ≥2-fold in Biolog PM cultures, suggesting utility as prebiotics and/or components of synbiotics.

4.2. Future Directions.

- Repeat 16S rRNA profiling of naive mice (for comparison to Bt-infected mice) after modifying the NGS library preparation protocol to prevent jack-pot effects.
    - Include dummy DNA template and/or combine airway DNA extracts from many mice in order to prevent runaway PCR amplification.
    - Success should enable publication of our 16S rRNA profiling studies of the airway microbiome in naive *vs* Bt-infected mice.
- Identify mechanisms of action underlying CP re-colonization of the mouse airway.
    - Identify genes mediating colonization *via* forward genetics (*i.e.*, gene deletion/overexpression screens *in vivo*).
- Identify mechanisms of action underlying CP inhibition of Bt *in vitro*.
    - Attempt to isolate cell/supernatant fractions displaying inhibiting activity and identify the compounds responsible *via* mass spectrometry.
    - Knock out genes predicted to mediate production of anti-bacterial compounds and determine whether the mutant CPs display diminished anti-Bt activity *in vitro*.
    - Engineer CPs to overexpress genes that mediate production of anti-Bt compounds and determine whether the mutant CPs display enhanced anti-Bt activity *in vitro*, and potentially also enhanced colonization and/or protection *vs* respiratory Bt infection.
- Identify additional examples of CP combinations that synergistically inhibit Bt *in vitro*, and determine whether such CP combinations provide better protection *vs* respiratory Bt infection (as compared to individual CPs).
- Determine whether varying CP culture conditions prior to administration to the airway can impact ability to re-colonize and/or provide protection *vs* respiratory Bt infection.
    - Test LB *vs* sSputum *vs* Biolog media that enhance CP (but not Bt) metabolic activity.
- Determine whether carbon sources (and potentially nitrogen sources) that enhance CP (but not Bt) metabolic activity in the Biolog system can serve as prebiotics (as evident from elicited protective effects *vs* respiratory Bt infection) and/or synbiotics (as evident from enhanced ability of CPs to re-colonize the airway and/or protect *vs* respiratory Bt infection).
- Identify mechanisms of action underlying CP-mediated protection *vs* respiratory Bt infection.

    - Does mechanism of action vary with CP?
    - Does mechanism of action vary with timing of administration (*e.g.*, 3 d *vs* 5 d *vs* 7 d prior to Bt challenge)?
    - Does the CP directly attack *vs* competitively exclude Bt? If the latter, is this accomplished by enlisting airway microbiome constituents, host cells, and/or host immune responses?
- Determine whether CPs (individually and/or in combination) can protect *vs* respiratory infection caused by other pathogens (*i.e.*, show broad spectrum activity *in vivo*).
    - Test both bacterial and viral respiratory pathogens.

REFERENCES

[1] Aiosa N, Sinha A, Jaiyesimi OA, da Silva RR, Branda SS, Garg N (2022) Metabolomics analysis of bacterial pathogen *Burkholderia thailandensis* and mammalian host cells in co-culture. ACS Infect Dis 8:1646-62. doi: 10.1021/acsinfecdis.2c00233.

[2] Barfod KK, Roggenbuck M, Hansen LH, Schjørring S, Larsen ST, Sørensen SJ, Krogfelt KA (2013) The murine lung microbiome in relation to the intestinal and vaginal bacterial communities. BMC Microbiol 13:303. doi: 10.1186/1471-2180-13-303.

[3] Scheiermann J, Klinman DM (2017) Three distinct pneumotypes characterize the microbiome of the lung in BALB/cJ mice. PLoS ONE 12:e0180561. doi: 10.1371/journal.pone.0180561.

[4] Kostric M, Milger K, Krauss-Etschmann S, Engel M, Vestergaard G, Schloter M, Schöler A (2018) Development of a stable lung microbiome in healthy neonatal mice. Microb Ecol 75:529-42. doi: 10.1007/s00248-017-1068-x.

[5] Dickson RP, Erb-Downward JR, Falkowski NR, Hunter EM, Ashley SL, Huffnagle GB (2018) The lung microbiota of healthy mice are highly variable, cluster by environment, and reflect variation in baseline lung innate immunity. Am J Respir Crit Care Med 198:497-508. doi: 10.1164/rccm.201711-2180OC.

[6] Schully KL, Bell MG, Ward JM, Keane-Myers AM (2014) Oropharyngeal aspiration of *Burkholderia mallei* and *Burkholderia pseudomallei* in BALB/c mice. PLoS ONE 9:e115066. doi: 10.1371/journal.pone.0115066.

[7] Wood DE, Lu J, Langmead B (2019) Improved metagenomic analysis with Kraken 2. Genome Biol 20:257. doi: 10.1186/s13059-019-1891-0.

[8] Lu J, Salzberg SL (2020) Ultrafast and accurate 16S rRNA microbial community analysis using Kraken 2. Microbiome 8:124. doi: 10.1186/s40168-020-00900-2.

[9] Lu J, Breitwieser FP, Thielen P, Salzberg SL (2017) Bracken: Estimating species abundance in metagenomics data. Peer J Comp Sci 3:e104. doi: 10.7717/peerj-cs.104.

[10] Cole JR, Wang Q, Fish JA, Chai B, McGarrell DM, Sun Y, Brown CT, Porras-Alfaro A, Kuske CR, Tiedje JM (2014) Ribosomal Database Project: Data and tools for high throughput rRNA analysis. Nucl Acids Res 42:D633-42. doi: 10.1093/nar/gkt1244.

[11] Lagier JC, Armougom F, Million M, Hugon P, Pagnier I, Robert C, Bittar F, Fournous G, Gimenez G, Maraninchi M, Trape JF, Koonin EV, La Scola B, Raoult D (2012) Microbial culturomics: Paradigm shift in the human gut microbiome study. Clin Microbiol Infect 18:1185-93. doi: 10.1111/1469-0691.12023.

[12] Lagier JC, Dubourg G, Million M, Cadoret F, Bilen M, Fenollar F, Levasseur A, Rolain JM, Fournier PE, Raoult D (2018) Culturing the human microbiota and culturomics. Nat Rev Microbiol 16:540-50. doi: 10.1038/s41579-018-0041-0.

[13] sourceforge.net/projects/bbmap/

[14] Bankevich A, Nurk S, Antipov D, Gurevich AA, Dvorkin M, Kulikov AS, Lesin VM, Nikolenko SI, Pham S, Prjibelski AD, Pyshkin AV, Sirotkin AV, Vyahhi N, Tesler G, Alekseyev MA, Pevzner PA (2012) SPAdes: A new genome assembly algorithm and its applications to single-cell sequencing. J Comput Biol 19:455-77. doi: 10.1089/cmb.2012.0021.

[15] O'Leary NA, Wright MW, Brister JR, Ciufo S, Haddad D, McVeigh R, Rajput B, Robbertse B, Smith-White B, Ako-Adjei D, Astashyn A, Badretdin A, Bao Y, Blinkova O, Brover V, Chetvernin V, Choi J, Cox E, Ermolaeva O, Farrell CM, Goldfarb T, Gupta T, Haft D, Hatcher E, Hlavina W, Joardar VS, Kodali VK, Li W, Maglott D, Masterson P, McGarvey KM, Murphy MR, O'Neill K, Pujar S, Rangwala SH, Rausch D, Riddick LD, Schoch C, Shkeda A, Storz SS, Sun H, Thibaud-Nissen F, Tolstoy I, Tully RE, Vatsan AR, Wallin C, Webb D, Wu W, Landrum MJ, Kimchi A, Tatusova T, DiCuccio M, Kitts P, Murphy TD, Pruitt KD (2016) Reference sequence (RefSeq) database at NCBI: Current status, taxonomic expansion, and functional annotation. Nucl Acids Res 44:D733-45. doi: 10.1093/nar/gkv1189.

[16] Alanjary M, Steinke K, Ziemert N (2019) AutoMLST: An automated web server for generating multi-locus species trees highlighting natural product potential. Nucl Acids Res 47:W276-82. doi: 10.1093/nar/gkz282.

[17] Ondov BD, Treangen TJ, Melsted P, Mallonee AB, Bergman NH, Koren S, Phillippy AM (2016) Mash: Fast genome and metagenome distance estimation using MinHash. Genome Biol 17:132. doi: 10.1186/s13059-016-0997-x.

[18] Jain C, Rodriguez-R LM, Phillippy AM, Konstantinidis KT, Aluru S (2018) High throughput ANI analysis of 90K prokaryotic genomes reveals clear species boundaries. Nat Commun 9:5114. doi: 10.1038/s41467-018-07641-9.

[19] Barfod KK, Roggenbuck M, Hansen LH, Schjørring S, Larsen ST, Sørensen SJ, Krogfelt KA (2013) The murine lung microbiome in relation to the intestinal and vaginal bacterial communities. BMC Microbiol 13:303. doi: 10.1186/1471-2180-13-303.

[20] Scheiermann J, Klinman DM (2017) Three distinct pneumotypes characterize the microbiome of the lung in BALB/cJ mice. PLoS ONE 12:e0180561. doi: 10.1371/journal.pone.0180561.

[21] Kostric M, Milger K, Krauss-Etschmann S, Engel M, Vestergaard G, Schloter M, Schöler A (2018) Development of a stable lung microbiome in healthy neonatal mice. Microb Ecol 75:529-42. doi: 10.1007/s00248-017-1068-x.

[22] Stevens MP, Haque A, Atkins T, Hill J, Wood MW, Easton A, Nelson M, Underwood-Fowler C, Titball RW, Bancroft GJ, Galyov EE (2004) Attenuated virulence and protective efficacy of a *Burkholderia pseudomallei* bsa type III secretion mutant in murine models of melioidosis. Microbiology 150:2669-76. doi: 10.1099/mic.0.27146-0.

[23] Gutierrez MG, Yoder-Himes DR, Warawa JM (2015) Comprehensive identification of virulence factors required for respiratory melioidosis using Tn-seq mutagenesis. Front Cell Infect Microbiol 5:78. doi: 10.3389/fcimb.2015.00078.

[24] Pilatz S, Breitbach K, Hein N, Fehlhaber B, Schulze J, Brenneke B, Eberl L, Steinmetz I (2006) Identification of *Burkholderia pseudomallei* genes required for the intracellular life cycle and *in vivo* virulence. Infect Immun 74:3576-86. doi: 10.1128/IAI.01262-05.

[25] Lazar Adler NR, Stevens MP, Dean RE, Saint RJ, Pankhania D, Prior JL, Atkins TP, Kessler B, Nithichanon A, Lertmemongkolchai G, Galyov EE (2015) Systematic mutagenesis of genes encoding predicted autotransported proteins of *Burkholderia pseudomallei* identifies factors mediating virulence in mice, net intracellular replication and a novel protein conferring serum resistance. PLoS ONE10:e0121271. doi: 10.1371/journal.pone.0121271.

[26] Arkin AP, Cottingham RW, Henry CS, Harris NL, Stevens RL, Maslov S, Dehal P, Ware D, Perez F, Canon S, Sneddon MW, Henderson ML, Riehl WJ, Murphy-Olson D, Chan SY,

Kamimura RT, Kumari S, Drake MM, Brettin TS, Glass EM, Chivian D, Gunter D, Weston DJ, Allen BH, Baumohl J, Best AA, Bowen B, Brenner SE, Bun CC, Chandonia JM, Chia JM, Colasanti R, Conrad N, Davis JJ, Davison BH, DeJongh M, Devoid S, Dietrich E, Dubchak I, Edirisinghe JN, Fang G, Faria JP, Frybarger PM, Gerlach W, Gerstein M, Greiner A, Gurtowski J, Haun HL, He F, Jain R, Joachimiak MP, Keegan KP, Kondo S, Kumar V, Land ML, Meyer F, Mills M, Novichkov PS, Oh T, Olsen GJ, Olson R, Parrello B, Pasternak S, Pearson E, Poon SS, Price GA, Ramakrishnan S, Ranjan P, Ronald PC, Schatz MC, Seaver SMD, Shukla M, Sutormin RA, Syed MH, Thomason J, Tintle NL, Wang D, Xia F, Yoo H, Yoo S, Yu D (2018) KBase: The United States Department of Energy systems biology knowledgebase. Nat Biotechnol 36:566-9. doi: 10.1038/nbt.4163.

[27] van Heel AJ, de Jong A, Song C, Viel JH, Kok J, Kuipers OP (2018) BAGEL4: A user-friendly web server to thoroughly mine RiPPs and bacteriocins. Nucl Acids Res 46:W278-81. doi: 10.1093/nar/gky383.

[28] Hammami R, Zouhir A, Le Lay C, Ben Hamida J, Fliss I (2010) BACTIBASE second release: A database and tool platform for bacteriocin characterization. BMC Microbiol 10:22. doi: 10.1186/1471-2180-10-22.

[29] Blin K, Shaw S, Kloosterman AM, Charlop-Powers Z, van Wezel GP, Medema MH, Weber T (2021) antiSMASH 6.0: Improving cluster detection and comparison capabilities. Nucl Acids Res 49:W29-35. doi: 10.1093/nar/gkab335.

[30] Davis JJ, Wattam AR, Aziz RK, Brettin T, Butler R, Butler RM, Chlenski P, Conrad N, Dickerman A, Dietrich EM, Gabbard JL, Gerdes S, Guard A, Kenyon RW, Machi D, Mao C, Murphy-Olson D, Nguyen M, Nordberg EK, Olsen GJ, Olson RD, Overbeek JC, Overbeek R, Parrello B, Pusch GD, Shukla M, Thomas C, VanOeffelen M, Vonstein V, Warren AS, Xia F, Xie D, Yoo H, Stevens R (2020) The PATRIC Bioinformatics Resource Center: Expanding data and analysis capabilities. Nucl Acids Res 48:D606-12. doi: 10.1093/nar/gkz943.

[31] Brettin T, Davis JJ, Disz T, Edwards RA, Gerdes S, Olsen GJ, Olson R, Overbeek R, Parrello B, Pusch GD, Shukla M, Thomason JA 3rd, Stevens R, Vonstein V, Wattam AR, Xia F (2015) RASTtk: A modular and extensible implementation of the RAST algorithm for building custom annotation pipelines and annotating batches of genomes. Sci Rep 5:8365. doi: 10.1038/srep08365.

[32] Ma J, Sun M, Pan Z, Lu C, Yao H(2018) Diverse toxic effectors are harbored by *vgrG* islands for interbacterial antagonism in type VI secretion system. Biochim Biophys Acta Gen Subj 1862:1635-43. doi: 10.1016/j.bbagen.2018.04.010.

[33] Bailey TL, Johnson J, Grant CE, Noble WS (2015) The MEME Suite. Nucl Acids Res 43:W39-49. doi: 10.1093/nar/gkv416.

[34] Bailey TL, Gribskov M (1998) Combining evidence using *p*-values: application to sequence homology searches. Bioinformatics 14:48-54. doi: 10.1093/bioinformatics/14.1.48.

[35] Das S, Bernasconi E, Koutsokera A, Wurlod DA, Tripathi V, Bonilla-Rosso G, Aubert JD, Derkenne MF, Mercier L, Pattaroni C, Rapin A, von Garnier C, Marsland BJ, Engel P, Nicod LP (2021) A prevalent and culturable microbiota links ecological balance to clinical stability of the human lung after transplantation. Nat Commun 12:2126. doi: 10.1038/s41467-021-22344-4.

[36] Knappe TA, Linne U, Zirah S, Rebuffat S, Xie X, Marahiel MA (2008) Isolation and structural characterization of capistruin, a lasso peptide predicted from the genome sequence of *Burkholderia thailandensis* E264. J Am Chem Soc 130:11446-54. doi: 10.1021/ja802966g.

[37] Li H, Han X, Dong Y, Xu S, Chen C, Feng Y, Cui Q, Li W (2021) Bacillaenes: Decomposition trigger point and biofilm enhancement in *Bacillus*. ACS Omega 6:1093-8. doi: 10.1021/acsomega.0c03389.

[38] Bochner BR, Gadzinski P, Panomitros E (2001) Phenotype microarrays for high-throughput phenotypic testing and assay of gene function. Genome Res 11:1246-55. doi: 10.1101/gr.186501.

[39] Khaledian E, Brayton KA, Broschat SL (2020) A systematic approach to bacterial phylogeny using order level sampling and identification of HGT using network science. Microorganisms 8:312. doi: 10.3390/microorganisms8020312.

[40] Khurana H, Sharma M, Verma H, Lopes BS, Lal R, Negi RK (2020) Genomic insights into the phylogeny of *Bacillus* strains and elucidation of their secondary metabolic potential. Genomics 112:3191-200. doi: 10.1016/j.ygeno.2020.06.005.

DISTRIBUTION

Name	Org.	Sandia Email Address
Joseph Schoeniger	8623	jsschoe@sandia.gov
Technical Library	1911	sanddocs@sandia.gov

This page left blank

Sandia National Laboratories

Sandia National Laboratories is a multimission laboratory managed and operated by National Technology & Engineering Solutions of Sandia LLC, a wholly owned subsidiary of Honeywell International Inc. for the U.S. Department of Energy's National Nuclear Security Administration under contract DE-NA0003525.